

## Nature of COX-2: Constitutive or Inducible, during the embryonic life of the domestic hen

### Agenda of this chapter

This chapter deals with a basic understanding of where COX-2 comes into picture during the embryogenesis of *Gallus domesticus*. The chapter starts with the introduction of COX enzymes, their already known biological functions, NSAIDs, their discovery and further innovation, as well as the basic morphological details about the organs of chick embryos, which may be helpful to understand the results of this chapter better. The discussion part of this chapter deals with correlating the results of this chapter with those of similar studies conducted in the world. It ends with the conclusion and snapshot summary of the inferences made out of the results of experiments.

### INTRODUCTION

The second isozyme of cyclooxygenases (COX), known as COX-2, had always been thought to be inducible until the mid-1990s when it was found to affect the bone formation process (Forwood, 1996; Klein-Nulend et al., 1997). These researches brought an initial idea that COX-2 could possibly have other roles to play than the inflammatory responses it was known to mediate. Subsequently, researchers utilised transgenic animal models for the identification of various functions of COX-2 in animal development and physiology (Oshima et al., 1996; Liu et al., 2001). The genes of COX-1 and COX-2 are located on different chromosomes and are often called *ptgs-1* and *ptgs-2*, respectively. This thesis, however, refers to them simply as COX-1 and COX-2 genes, which are synonymous with *ptgs-1* and *ptgs-2* (birdgenenames.org).

COX-1 and COX-2 functional compensation is a topic of debate over the years. In the COX-1 null mice, uterine permeability was hampered until COX-2 expression increased and rescued the process, showing the delayed functional compensation (Reese et al., 1999). However, the failed implantation in COX-2 deficient mice could be secured neither by COX-1 nor by exogenous PGE<sub>2</sub> (Li et al., 2018). The compensation of isoforms is still not proven

with mechanistic details. Nonetheless, in non-mutant normal organisms, these isoforms perform some unique functions, which are not compensated by the other isoform. In these circumstances, the naturally increasing levels of the other isoform do not relieve the system from the loss occurred due to inhibition of one isoform. The list of such functions is given in the section below.

## **1. Neuroinflammation**

The process of inflammation occurring in the nervous system components is called a 'neuroinflammation' (Choi et al., 2009). Neuroinflammation is like a defense mechanism if controlled timely. Nevertheless, excessive neuroinflammation causes damage to the tissues experiencing it. A normally functioning nervous tissue always requires a constant basal level of this process. A normal nervous tissue also exhibits a surge in this process while attempting a fight against central nervous system (CNS) injuries. Simultaneous action of repairing genes allows the tissue to heal from damage. An innate immune response in CNS is mediated by microglial cells in mammals (DiSabato et al., 2016). Usually, COX-1 acts as a constitutively expressed housekeeping gene, and COX-2 is upregulated in inflammation in all the tissues of the body. However, COX-1 is found to be expressed more in microglia rather than COX-2 during neuroinflammation (Choi et al., 2009). The well-known inflammatory COX-2 is still thought to be participating in neuroinflammation, and most of the neurological disorders are managed using COX-2 specific NSAIDs. These include Parkinson's disease, multiple sclerosis, amyotrophic lateral sclerosis, neuropathic pain, and cerebrovascular disease (Terzi et al., 2017). However, in reality, COX-1 is found to be producing prostanoids in the activated microglia way ahead of the upregulation of COX-2 (Choi et al., 2009).

Several other COX-1 functions are coming up as research progressed in this field in the past decade. It is now globally known that COX-1 induced PGD<sub>2</sub> elevates the severity of the pathophysiology of spinal cord nerve injury (Kanda et al., 2013). It also elevates the pain in neuropathy and peripheral hypersensitivity (Kanda et al., 2013). The process of aging is also related to the susceptibility of nervous system components (especially brain) to the inflammatory damage. This process is also mediated by COX-1 induced TXB<sub>2</sub> (Bosetti and Choi, 2010). Owing to these works and their results, COX-1 specific drugs are thought to be more useful to combat the neuroinflammatory conditions in humans (Bosetti and Choi, 2010). Such studies also reveal the paradox of the nature of these COX isoforms.

## 2. Gastrointestinal Cavity Integrity

The gastrointestinal (GI) cavity is known to be protected by the products of COX-2 for a long time because of the ulceration which occurred while using COX-1 specific pain killers. The functional detail of such a process lies right in the physiological details about the GI cavity. GI cavity is lined by mucosa layer consisting of smooth muscle cells and epithelial cells embedded in connective tissue – lamina propria (Hickman, 1961). Lamina propria is lined further by mucus cells, which are arranged in several layers toward the cavity. These mucus cells secrete bicarbonate and mucus, which protect all the interior components of the GI wall, by neutralizing the pH (Forsell, 1988). When the long-term exposures to non-specific NSAIDs caused lesions in the GI wall, damage to mucus cells was a suspected reason in the case (Halter, 2001). Immunolabelling of GI wall cells showed the presence of COX-1 in these cells. Inhibition of COX-1 via specific inhibitor SC-560 hampered the mucus-bicarbonate barrier synthesis, and the GI wall got affected by acidic and noxious agents (Halter, 2001). Further investigations showed that there was a reduced blood flow passing through enteric mucosa in such experimental animals (Halter, 2001). The reduction in blood flow also reduces the supply of oxygen and nutrients to the local cells. It also hinders the process of getting rid of harmful agents and hydrogen ions (Forsell, 1988). Another strategy of mucosal defense is via PG secretion. The 'cytoprotection' provided by PGE<sub>2</sub> and PGI<sub>2</sub> is mediated via COX-1 enzyme (Takeuchi and Amagase, 2018). These are the prostanoids behind the increase in the blood flow via a reduction in the arterial blood pressure (Whittle, 1980; Takeuchi and Amagase, 2018). PGE<sub>2</sub> also acts on enterochromaffin-like (ECL) cells to decrease the acid output (Kato et al., 2005).

In this manner, inhibition of COX-1 affects GI integrity. In this case, the repair mechanisms drag along the COX-2 pathway. The inflammatory mechanism provoked due to the wall damage, and lesions are suppressed with the help of COX-2 (Fu et al., 1999). TX, a product of COX-2 activity, is known to stop excessive bleeding by activating the clotting pathway (Halter et al., 2001). COX-2 positively regulates neovascularization, which helps the supply of nutrients in the local niche of damaged tissue (Kim et al., 2001). Therefore, the wound healing process cannot proceed without the upregulation of COX-2. However, COX-2 specific or non-specific NSAIDs hamper COX-2 activity along with the limited or high suppression of COX-1 activity, respectively. The COX-1 specific NSAID causes the initiation of GI wall damage and ulceration. COX-2 specific ones can lead to heightened

ulceritis by slowing down the healing process. Therefore, initially discovered NSAIDs, which used to inhibit COX-1 and COX-2 both, led to damage to a greater extent.

### **3. Cardiovascular System**

The major component of the cardiovascular system – the heart, always bears the basal level of COX-1 protein in the blood vessels and endocardial cells. However, COX-1 is not immunolocalized in the cardiomyocytes, which are localized with COX-2 protein (Zidar et al., 2007). Thus, when heart sections are localized with antibodies specific to COX-1, the whole tissue shows the high and diffused presence of COX-1 antigen. The same sections localized with COX-2 antibody show the fluorescence in rather smaller patches (Zidar et al., 2007). The primary function performed by COX-2 herein is the protection of cardiac tissue from ischemic insult, which otherwise causes a momentary lack of oxygen to cardiac cells leading to injury. Cardiac cells combat via early and late mechanisms, including ischemic preconditioning and recovery, respectively. The recovery phase is the result of two PGs – PGE<sub>2</sub> and PGI<sub>2</sub> derived by the action of COX-2 (Bolli et al., 2002).

The vasodilation and vasoconstriction are also regulated via the action of PGs in the whole body of organisms. PGI<sub>2</sub> inhibits platelet aggregation by dilating the blood vessels (Majerus, 1983). It is produced by the endothelial cells of blood vessels in response to the stimulus provided by bradykinin and histamine via the activity of COX-1 (Majerus, 1983; Liu et al., 2012). COX-1 performs the opposite function of constricting vessel derived TXA<sub>2</sub>. The hypoxic condition triggers COX-2 rather than COX-1 for the similar function of prostanoids, including PGI<sub>2</sub> and TXA<sub>2</sub> (Delannoy et al., 2010). Mainly in the hypoxic condition, 8-iso-PGF<sub>2α</sub> is upregulated, which in turn decreases PGI<sub>2</sub> secretion from the pulmonary arteries (Delannoy et al., 2010). Therefore, later on inhibition of TP (thromboxane prostanoid) receptor was proposed as a strategy to manage hypoxia (Janssen, 2008).

In summary, COX-1 and COX-2 act as essential enzymes in numerous vasculo-motor actions in organisms. Deranged biosynthesis of prostanoids due to the irregular levels of COX enzymes leads to several cardiovascular diseases. Atherosclerosis, Prinzmetal Angina, myocardial infarction – are all examples of such disorders. Additionally, increased COX-2 activity leads to rhinitis, dermatitis, and other common allergic reactions as well in different circumstances (Rucker and Dhamoon, 2020).

## **4. Kidneys**

Limited information is available about the genesis of the kidneys involving COX pathways. However, COX-2 deficient mice do not develop normal kidney architecture, provided they survive more than six months of their ages (Dinchuk et al., 1995; Sellers et al., 2010). This experiment suggested a plausible function of COX-2 in kidney formation in the embryonic life of mice. Moreover, both the COX isozymes are found in the adult kidneys as well, indicating their role in the maintenance of routine kidney functions.

A kidney is the functional unit of the excretory system in organisms. Out of all the excretory material that it helps the body to get rid of, prostanoids are some excreted materials as well. PGE<sub>2</sub> is excreted the most out of all the prostanoids that are eliminated by the kidney (Li et al., 2018). During the process of elimination, PGE<sub>2</sub> participates in the essential physiological phenomenon – osmoregulation. It assists the nephrons in ultrafiltration and sodium transport (Kim, 2008). PGI<sub>2</sub> can modulate glomerular filtration rate (GFR), and PGE<sub>2</sub> can modulate salt-water transport along the Henle's loop in accordance with the needs of physiology at various instances (Goetz Moro et al., 2017). These functions have been associated to COX-2 activity because research suggests that only the second isoform of COX is predominantly present in the ascending loop of Henle (Goetz Moro et al., 2017). Conclusively, COX enzymes have less known functional aspects in the development and maintenance of the kidney and its functions, respectively.

## **5. Cancer**

Its suspected association with cancer is the reason why COX-2 studies gained momentum beginning the last decade. NSAIDs have started to be proven as wonder drugs, as they worked well for treating the diseases of inflammatory, neurodegenerative, cardiovascular, and many more kinds – to which Cancer is a more recent addition. COX-2 was found to be overexpressed in the tumors of the endometrium (St-Germain et al., 2004), breast (Parrett et al., 1997), prostate (Gupta et al., 2000), and colon (Jang et al., 2009). In some experiments, when COX-2 is genetically overexpressed, the animals developed metastatic tumors at a greater rate (Liu et al., 2001). It was in 1986 when COX-2 was proven for the first time as a mediator to the human oesophageal tumorigenesis (Botha et al., 1986). Once COX-2 was known to be mediating, the underlying mechanisms were dug upon. It was found that out of

four major prostanoids - PGE<sub>2</sub> and PGF<sub>2α</sub> were higher in the tumors as compared to the normal cell clusters (Pannunzio and Coluccia, 2018). Probably this kind of research led to the usage of NSAIDs (specifically COX-2 inhibitors) as anti-cancer medicines.

COX-2 selective inhibitors have been known to inhibit carcinogenesis in established tumors (Thun et al., 2002). They also enhance tumor suppression in the model organisms with sporadic colorectal adenomas (Harris et al., 2000). Studies often show that NSAIDs inhibit tumor progression by two main mechanisms – 1. by upregulating the apoptotic genes and 2. by downregulating the angiogenic genes (Thun et al., 2002). Very few animal experiments and a large number of epidemiological studies have found that NSAIDs do not have severe side effects such as colorectal adenomatosis or Cancer (Pinczowski et al., 1994; Schreinemachers and Everson, 1994). Nonetheless, some researchers contradict the idea of safe long-term usage of NSAIDs (Paganini-Hill et al., 1989; Paganini-Hill, 1995).

All of the abovementioned functions of COX enzymes were known either via the development of transgenic models lacking one or both normal COX genes, or via the usage of NSAIDs. NSAIDs have an interesting history, as mentioned in the 'Introduction' section. They were very much in use when their mechanisms were not known at all. Today, NSAIDs are the most prescribed medicines across the globe (Wongrakpanich et al., 2018).

### **Discovery of NSAIDs in Brief**

Felix Hoffman, working on drug development in Bayer's company, was finding a way to decrease the oral toxicity of Salicylic acid (Miner and Hoffhine, 2007). His father, a patient of rheumatoid arthritis, was consuming Salicylic acid in powder form to combat the pain (Brune and Hins, 2004). He modified the basic structure of Salicylic acid by deriving an idea from C. F. von Gerhardt during a literature survey (Brune and Hins, 2004). The new drug – acetylsalicylic acid was named as 'aspirin' ('A' for Acetylation and 'spirin' for *Spiria* – a genus of shrub used for procuring salicylic acid). The very next year of its synthesis, Heinrich Dreser at Bayer company dropped the idea of selling aspirin anymore, saying that it showed 'enfeebling' action of the heart, and it had no market value anymore. However, he did that because of his anticipation towards the sale of 'heroin' synthesized by Bayer laboratory as a remedy for cough (Sneader, 1998). Arthur Eichengruen, appointed in Bayer to originate the novel drugs, did not support the dismiss of aspirin and pushed Hoffman for aspirin

production (Pearce, 2014). Eventually, Dreser was the subject for checking the effect of produced aspirin along with the rabbits. Finally, aspirin was in the market, proving its more tolerable side effects than Salicylic acid (Dreser, 1899). Fortunately, the acetylated form was found effective in preventing coronary and cerebral thromboses (Craven, 1952). The highly efficient aspirin and then developed similar NSAIDs became popular in no time. Their increased usage started to cause ulceration and aplastic anemia in the patients (McCarthy and Chalmers, 1964; Hudson and Hawkey, 1993; Wallace, 2000). Therefore, as soon as the mechanism of aspirin's action was known, studies were conducted to develop COX-2 specific drugs rather than non-specific COX inhibitors (Hawkey, 1999).

One of the NSAIDs – Etoricoxib was used for this work. It was patented in 1996 and was approved for medical use in the year 2002 (Ganesan and Proudfoot, 2010). It was added to the embryos at a fixed interval of time, and the effects were evaluated at morphological, molecular, anatomical, and metabolomic levels post initial pharmacokinetic study for RIR chicks.

### **Basic Morphological Features of Chick Embryo**

The anatomical features focussed in this research include somites, notochord, nerve cord, craniofacial structures such as the head (and compartments), eyes, beak, egg tooth, heart, limbs, feathers, and vasculature.

Chick embryo inside a freshly laid egg contains about 50-60 thousand cells. These are arranged in multiple layers collectively known as blastoderm within three hours, with or without the optimum temperatures and humidity parameters. A stage preceding this bears a blastodisc, which is a single layer of cells (Kotpal, 2010). The embryo at zero hours (unincubated, freshly laid) is visually a union of two concentric circles when watched from the top. The circle lined by the interior ring of two concentric rings is made up of cells, which transmit more light that falls on them. These cells make area pellucida (figure 4), which will eventually form the embryo proper as and when the development pass through several stages. The outer edge of area pellucida is made up of darker cells making up a thick bank-like area called an area opaca (as the layer is opaque) (figure 5A). Area opaca forms the extraembryonic membranes. Just in a day, the embryo develops several structures, namely – primitive streak, Hensen's node, head fold, and a somite (figure 5B). Somites are epithelially

packaged mesodermal pockets. They are also present in other vertebrates during embryogenesis (Pourquié, 2018).

Somites act as the stage-determining characteristic for chick embryos until HH 10 (32 to 38 hours), because then after the first somite begins to dwindle (Hamilton and Hamburger, 1951). Day-1 is therefore marked by one somite and day-2 by the presence of optic vesicle as well as optic stalk. Some of the HH stages have overlapping time points in terms of hours or days. For instance, HH 12 and HH 13, both have common time points of 48 and 49 hours. Therefore, the embryos isolated precisely at 48 and 49 hours of incubation, could differ in characteristics depending upon small variation in either of the factors such as – lag in placing embryos in an incubator, minute temperature variations among the compartments of the same incubator, small variations in humidity or any other factors that could affect the early developmental events naturally. HH 13 is characteristically different from HH 12 since the embryo starts to take a turn at the junction of brain compartments and somites (figure 6). From the third day onwards, limb bud grows significantly each day, which provides a good criterion for identification of developmental stages till day-9 (figures 7 to 10). Along with limbs, visceral arches also show variations in morphology each day from 4 to 9, which also work as a reliable characteristic for the identification of stages. However, for using visceral arches as a criterion, one needs a simple microscope to get a detailed idea of structure, while limbs can be observed by naked eyes for the same. From day-9 to day-12, eyelids and feather germs act as criteria observable with naked eyes along with some changes in hindlimb autopods. The authors, Hamilton and Hamburger, for the division of later stages than day-12 use the increase in the size of each organ as the only criteria. Because, all the structures are already formed till day-12 and just show significant growth in dimensions until a chick hatches on or around day-21 of incubation (Hamburger and Hamilton, 1951). Therefore, this research particularly focuses on days 1 to 12, wherein all the primitive organogenesis is completed, and the stages are well divided based on the state of these organs' development. Among these also, day-8 may contain characters as described to be of HH 34 or HH 35. That said, the day-8 embryo may or may not show the nictitating membrane moved closer to scleral papillae, which is a characteristic of day-9 embryos instead (Hamburger and Hamilton, 1951). Day-8 and day-9 embryos are overall similar to each other (figures 9 and 10). Day-8, however, still shows a thin web between digits, which is absent after day-9. More closely and characteristically, a completely looped heart bearing the atria on the top of ventricles can be well-observed at day-4 for the first time in the growing chick embryo. All

the three parts of limbs – stylopod, zeugopod, and autopod are visible from day-5 of incubation.

## **METHODOLOGY**

The agenda of this chapter was to ascertain the nature of COX-2, whether constitutive or inducible, during the embryonic life of the chick of the domestic hen. To establish the nature, the basal level of COX-2 in various tissues of the chick embryo seemed necessary. The embryonic development partially finishes organogenesis in the phase between day-0 to day-10, after which the growth of all organs occurs to make the chick ready to hatch. Therefore, the study design was limited to isolation in the main organogenic phase day-1 to day-12. Day-0 embryo was not included in gene expression and protein level studies due to the atypical deviation in the stage characteristics depending upon the weather and minor delay (1-3 hours) in the collection of eggs from the poultry unit.

The collected eggs were first wiped with an antibiotic solution, and the egg incubator was sterilized beforehand. The eggs were divided into the control and experimental groups as per the experiment type. The treatment was carried out using an air cell method as described in the chapter-2 of the thesis, which also describes a detailed methodology for each of the experiments mentioned in this chapter. First of all, the test chemical etoricoxib was dissolved in various solvents to identify the appropriate solvent with the least toxicity. The dissolved test chemical was then added to the embryos to perform the dose range analysis. This experiment derived one dosage that was to be added to embryos in all other following experiments. The mortality observed in the dose range analysis was confirmed to be due to etoricoxib. This confirmation was inferred from the results of LC-MS of etoricoxib performed in control as well as experimental embryos. Once the etoricoxib was found reaching embryos, the COX activity assay was performed to check the extent of activity reduction due to etoricoxib. This experiment was, therefore, carried out in both the control and experimental groups. It was now known that COX-2 activity was reduced significantly in treated embryos when compared with control embryos. Therefore, the presence of the COX-2 gene and protein in these embryonic tissues was checked next using qRT-PCR and western blotting techniques. Lastly, COX-2 was immunolocalized in chick embryos to derive a conclusion about the nature of COX-2 in the embryonic life of domestic hen.

## RESULTS

### Standardization of Etoricoxib Vehicle

Etoricoxib being sparingly soluble in water, as well as in oil, the vehicle used for the current work, was decided after using several solvent compositions in the embryos. The results are presented in the table 6. Here, the eggs were first treated with only the solvent mixtures and the mortality was checked at HH 24 (day-4). The live embryos possessed the beating hearts, which discriminated them from the dead embryos showing no such movements. The embryos added with DMSO and PBS mixture showed a significantly high mortality rate without the addition of etoricoxib itself.

On the other hand, after being proven as non-toxic to the chick embryos, the solvents were added with etoricoxib. The same concentration of etoricoxib 100 µg/mL (decided from earlier study as per the average weight of eggs, Buch et al., 2018) was used in all the cases to check the difference between the efficacy of solvents to carry the test chemical to the embryos. This part of data showed that some solvents along with etoricoxib synergistically increased the death rate of young embryos (isolated at HH 24, day-4). PEG-400, whether dissolved in water or PBS, caused higher mortality in the embryos. DMSO led to more deaths in embryos in both PBS and water as well. Etoricoxib dissolved in CMC (prepared in water) was found on the membrane as white precipitate-like matter when the eggs were opened for embryo isolation. None of the embryos died in this CMC-water-etoricoxib mixture. This kind of effect could be due to the permeability difference of various solvents through the shell membrane present between the air cell and egg contents. Viscous material or particulate components may take longer than the water-soluble one as the membrane is a simple meshwork of glycosaminoglycans and proteins, permeable to water (Ruff et al., 2009). Overall, the water acted as the best solvent due to a negligible mortality rate when added alone and proper carriage of etoricoxib to the embryo (table 6).

A dose-range study was performed for the etoricoxib solution prepared in water, which gave the dose-response data and was used further for determining the treatment concentration for all the experiments.

## **Dose-Range Study**

This study revealed that the mortality rates in chick embryos treated with etoricoxib (dissolved in water) increased with the increasing treatment concentration. The embryos treated with only water showed an average of 95 to 100 % survival, similar to an average 96 % survival rate of untreated embryos (table 7). The treatment of 10 µg/mL etoricoxib did not make any significant change in the survival rate (table 8). The addition of 50 µg/mL etoricoxib caused about 10 % mortality, which was still not a significant drop. The next concentrations starting from 100 to 500 µg/mL, caused massive mortality in embryos (table 7). Almost all the embryos died at a concentration of 500 µg/mL (figure 12).

Non-linear fit analysis and LD<sub>50</sub> was computed to be 144.4 µg/mL (10.01, 99.27) etoricoxib. Experimentally when the mortality for intermediate concentration 70 µg/mL was calculated, it was found to be around 30 %. In a subsequent computational analysis, it was found that 72.2 µg/mL was the lowest observed effect concentration (LOEC) and was therefore chosen for all further experiments. The activity of COX-2 (since etoricoxib is COX-2 specific inhibitor) was used for deciding the pattern of dosing, meaning the timepoints of treating eggs.

## **Liquid chromatography – Mass Spectroscopy of Etoricoxib**

The eggs were administered with a single pre-decided dose of etoricoxib (72.2 µg/mL) and were isolated at day-2 to check for the presence of the test chemical using LC-MS technique. Results showed that experimental embryos showed the mass peak of etoricoxib when acquired in positive mode. The control group embryos did not have any matching peaks eluting at the same time frame from the LC column. The treatment peak matched the standard solution peak when m/z and elution times were compared.

The standard solution LC profile shows up the peak of etoricoxib eluted at about 6 minutes (figure 13A). The confirmation of the peak belonging to etoricoxib was done using an m/z peak at 359 (figure 13B), which was derived in a positive mode, as discussed earlier. The molecular weight of etoricoxib is 358. Other tiny peaks visible in the spectrum in figure 13B can either be of the impurities in the solvents, test chemical, and/or poorly cleaned column. The largest peak has to be a mass peak of etoricoxib, as it is the standard solution made from etoricoxib and solvent. This similar timepoint, when magnified in the LC profile,

showed a peak in the experimental group as well. Here, in the treated embryonic homogenate sample, a peak of 359 appeared at 6 minutes, as shown in figure 13A. The control group spectra showed numerous small peaks and one high-intensity peak, which was 243 m/z. This peak eluted between 4 to 7 minutes but not anywhere close to 6 minutes (figure 13E and 13F). Certainly, this peak did not belong to etoricoxib, confirming that the embryos inherently did not possess the chemical showing peak exactly where etoricoxib does at the same LC timepoint. Thus, the existing peak in the treated group was confirmed to be an etoricoxib mass-peak.

The confirmation of etoricoxib penetration led to the next experiment, which depicted the difference in control and treated COX activity profiles, thereby providing detail about etoricoxib function.

### **COX-Activity Assay**

Administration of LOEC (72.2  $\mu\text{g/mL}$ ) dose of etoricoxib to the day-0 embryos decreased overall COX activity and also changed individual COX isozyme activities as well. These changes were measured until 10 days from day-1 embryos. The preparation of sample for each stage was done as described in chapter-2.

In the control scenario, total COX activity was highest on day-1. COX-2 activity at this timepoint was highest as compared to other time points as well. However, COX-1 activity remained close to zero (negligible). With the passing stages, total COX activity, as well as COX-2 activity, decreased till day-4 and then increased to a smaller extent till day-10. All these embryos showed almost no COX-1 activity (Figure 14A). The total COX activity was contributed only by COX-2 in the control embryos. The least COX activity was observed at day-4.

Experimental embryos, on the other hand, contained overall diminished activity of COX. COX-1 did not remain negligible in these embryos. The periodic upregulation of COX-1 activity coincided with the drastically decreasing COX-2 activity. These instances were noticed on day-2, day-6, day-9, and day-10. Etoricoxib – mediated COX-2 activity inhibition led to an increase in COX-1 activity. Nonetheless, the total COX activity made up by the activity of both these isoforms, was still less than that of the control embryos. The

significance values derived from three replicates and ANOVA (Chapter-2) are placed in table 9.

### **Gene Expression of COX in Control Embryos**

Absolute quantification of COX-1 and COX-2 transcripts was carried out in day-1 to day-10 control embryos to understand the basal level of their expression in the embryos. Interestingly, as mentioned previously, even though the activities of COX were found changing throughout these days, their expression levels remained more or less the same except for one stage, wherein COX-2 expression peaked.

DNA standards containing copy numbers – 100, 2000, 10000, 100000, 1000000 – were run in the typical qRT-PCR protocol as described in the chapter-2. These standards were provided along with the Roche LightCycler96 instrument. The average of three Cq was derived from three technical replicates. These readings, when plotted against the copy numbers added initially to the reaction, gave a standard graph and equation ( $R^2 = 0.9977$ ; figure 15).

The transcript numbers in the cDNA sample prepared from 1  $\mu$ g RNA was close to 3000 for both COX-1 and COX-2 in all the stages except for one. At day-9, COX-1 copy numbers remained steady like they were during all other days so far till day-9. However, at this timepoint, COX-2 copy numbers increased suddenly. The experiment was repeated thrice technically from three biological replicates each time. The data showed a similar pattern of the hike at day-9 in all the replicates. Overall, gene expression analysis showed that there was the least modulation in the copy numbers of transcripts of COX enzymes in the chick embryos (table 10). The data differed from the protein analysis, as described in the following segment.

### **Western Blot of COX in Control Embryos**

The level of proteins of COX-1 and COX-2 were checked using the western blot technique. The primary monoclonal antibodies and isotype-specific secondary antibodies were used to localize the proteins on PVDF membranes containing the transferred proteins. The proteins were transferred using a semi-dry blot technique. The results showed drastic differences from

those of gene expression patterns of the same genes. Nonetheless, they were quite relatable to the activity patterns of these proteins.

COX-1 protein remained less than COX-2 from day-1 to day-10 in control chicks except for one instance. At day-4, COX-1 and COX-2 protein concentration were similar to each other (table 11). Their concentration was close to each other on day-3 as well. Both COX-1 and COX-2 were at their respective peaks on day-1. COX-2 was the least concentrated on day-4 after the levels dropped sequentially from day-1 till this timepoint. After day-4, it started increasing slowly till day-10. COX-1, on the other hand, decreased from day-1 to day-4 and showed almost steady levels afterward till day-10 (figure 17). COX-1 and COX-2 protein levels differed from each other significantly overall (table 12). The discrimination between gene expression and protein levels of COX isozymes are discussed in detail in the discussion section.

### **Immunolocalization of COX-2 in embryos**

Understanding of presence of COX-2 in chick embryos was incomplete without its tissue level localization. This was performed using the colorimetric reaction-based immunolocalization of COX-2 in the chick embryos, starting from day-1 to day-10. The results revealed that COX-2 is present throughout the embryos, in various locations. It especially got localized in the growing tissues at the respective stages. For instance, COX-2 was found to be present in the limbs during its peak lengthening timepoint, i.e. days 5 to 8, specifically in the growing bones. The representative images showing where COX-2 localized primarily in each stage are discussed in this segment.

Day-1 embryos showed dispersed localization of COX-1. Here, at somites and optic vesicle, it was densely located (figure 18). Its dispersion reduced in day-2, wherein it became more specifically located surrounding somites and on the outer edge of the heart tube (figure 18). At this stage, the heart tube is normally still in a migration state. At day-3, it was found all over in the longitudinal section of the embryo. However, it got localized more densely near the developing eye, in the head, as well as in allantoic vesicle (figure 19). Heart tissue at day-4 showed the presence of COX-2, which showed complete folding of the heart tube at this stage. COX-2 got more localized in the walls of the heart (figure 19). The rapidly growing limbs showed the presence of COX-2 on day-5 near the areas of cartilage

condensation (bone formation). Both hindlimb and forelimb also bore COX-2 in the epithelium (figure 20). Day-6, when kidney cells differentiate, showed the presence of COX-2 in the kidney. Here, it also got localized in somites as well as in the tail region. The tail is the region which elongates the embryo body further from this stage (figure 20). COX-2 localization areas shrunk after this stage to very specific areas in the embryos in lower intensity. Day-7 embryo showed COX-2 localized near growing notochord (figure 21A). Growing testis showed the presence of COX-2 in seminiferous vesicle regions, as seen in the transverse section of the day-8 embryo (figure 21B).

Further, nerve cord and somites were immunolocalized with COX-2 in day-9 (figure 21C and 21D). Overall, the tissues which were growing the most rapidly at a particular stage showed higher COX-2 in them precisely at that stage. The localizations were confirmed not to be a background coloration by placing antibody controls parallelly handled in the similar way as all the other tissues were (figure 22).

## **DISCUSSION**

Cyclooxygenase enzymes have been the subject of considerable research since they were first identified as the targets of many of the most popular and best-known anti-inflammatory drugs. Two COX isoforms (COX-1 and COX-2) have been identified and, in addition to their well-known roles in inflammation, they have also been found to participate in a plethora of other biological processes, ranging from ovulation and fertilization to aging and death (Lim et al., 1997; Stanfield et al., 2003). One of the goals of this study was to explore the role of COX-1 and COX-2 in embryogenesis. While a small handful of studies have been published, relatively few have looked at the differing roles of COX isotypes and the effects of their downstream effectors on the development of multiple organs and tissues. To explore this aspect more thoroughly, we systematically studied the temporal and spatial tissue expression of both COX-1 and COX-2 in early (1 to 10 days) chick embryos. We also correlated induced changes in COX-2 activity with detectable embryo defects, as discussed in later chapters.

In vertebrates, COX-1 isozyme is constitutively expressed, while COX-2 is an inducible isotype that responds to inflammatory signals. However, based on the results of the current study, COX-2 appears to be expressed constitutively during normal chick embryogenesis. Our study has also revealed that the activity of COX-2 is unique for any

given day of development and that this activity varied temporally in the embryonic tissues. This suggests the constitutive nature of this isoform. A clear temporal trend in COX-2 protein levels was seen in embryos from day-1 till day-10 of their development when all the cellular events that culminate in organogenesis occur in chicks. The concentration of this protein in whole embryo extracts was highest on the first day of in-ovo development, followed by a steady decline until day-4 and then a weak upward trend up to day-10. In contrast to the protein levels, COX-2 mRNA showed relatively constant levels throughout these 10 days. This differing pattern in protein and transcript abundance is typical of a protein that is not subject to induction at the level of gene expression (Stanfield et al., 2003). Our result with chick embryos, however, contrasts with the data reported in mouse embryos, wherein organogenesis stages, i.e., gestational days 7 to 13, do not show the presence of COX-2 (Stanfield et al., 2003). On the contrary, some reports suggest that COX-2 is required for ductus arteriosus closure and nephrogenesis in mice and rats (Zhang et al., 1997; Loftin et al., 2001).

As highlighted in this study, we could locate COX-2 in embryonic somites, heart, brain, eyes, and the neural tube during the early chick embryonic development. Moreover, the inhibition of COX-2 caused anomalies, which are discussed in chapter-5 along with the correlation to COX-2 localization. Western blot analysis and other biochemical assays in the untreated control embryos revealed an apparent increase in the concentration as well as the activity of COX-2 during the first and second days of embryogenesis compared to the rest of the time points studied. These findings further reaffirm the role of COX-2 in chick (and likely in other vertebrates) development.

Several other published studies have focussed on the roles of COX-2 in mice embryogenesis using knockout models. These studies found that mouse embryos acquiesce in the absence of the COX-2 gene and develop without showing patent ductus arteriosus (Loftin et al., 1999). The authors suggested that the compensatory role of COX-1 might have allowed the embryos to survive without the ductus arteriosus closure defect. Therefore, the compensatory action of COX-1 was checked in our chick embryo model by studying its activity along with that of COX-2, in both the control and etoricoxib-treated groups. COX-1 activity increased when the embryos were challenged with the COX-2 antagonist, etoricoxib, which partially compensated for the total cyclooxygenase activity until day-3. However, day-4 experimental embryos experienced a partial revival of COX-2 activity. This kind of recovery can be either due to the elimination of etoricoxib by embryonic metabolism, or the

generation of new COX-2 protein. In any case, such an increase in COX-1 activity combined with a measurable decrease of COX-2 activity has been described for the first time in any tissue. Research suggests that PGs do not interfere in compensatory mechanisms of COX isozymes in-vitro using mouse lung fibroblasts (Vichai et al., 2005). They also confirmed the positive regulation of COX-2 by PGE<sub>2</sub> and PGF<sub>2α</sub> in the same system, which could be a plausible mechanism of action for the reactivation of COX-2 in treated chick embryos. However, the identification of the vital mediator molecules for heightened COX-1 activity needs further experimentation. In an effort to extend our study to identify the functional compensation of COX-2 by COX-1, we measured the levels of their downstream effectors – the prostanoids, as discussed in the chapter-4.

The experiments making this particular chapter helps one reach to the conclusion about COX-2 being constitutive as well as inducible in nature in embryos. It shows that COX-2 localized in various tissues during their growing stage must be involved in organogenesis. The inhibition was therefore planned to evaluate further, the systems which are affected due to COX-2 non-functionality in chick embryos.

## TABLES

Treatment mixture	Mortality rate (in %) without etoricoxib	Mortality rate (in %) with 100 µg/mL etoricoxib
0.01% PEG-400 in water	25	40
0.01% CMC in water	06	01
0.01% DMSO in water	35	52
0.01% PEG-400 in PBS	42	50
0.01% CMC in PBS	20	18
0.01% DMSO in PBS	72	85
PBS	08	56
Water	02	50

*Table 6: Standardization of vehicle for etoricoxib. The mortality rates are expressed as percentage. Water proved to be the best vehicle carrying etoricoxib with the least side effects.*

Dose (µg/ml)	% Survival (three replicates)			Average
Untreated	99	94	95	96
0 (vehicle control)	100	93	96	96
10	99	94	93	95
50	93	89	88	90
100	55	56	55	55
150	39	40	39	39
200	39	41	42	41
250	38	36	35	36
300	31	33	36	33
350	30	31	30	30
400	29	28	20	26
450	21	21	22	21
500	12	10	11	11

*Table 7: Dose-range analysis of etoricoxib in chick embryos. n = 3 technical replicates of 30 biological samples each.*

ANOVA table		SS	DF	MS	F (DFn, DFd)	P-value
Treatment (between columns)		30716	12	2560	F (12, 26) = 392.8	P<.001
Residual (within columns)		169.4	26	6.517		
Total		30885	38			
Dunnett's multiple comparisons test	Mean Diff.	95.00% CI of diff.	Significant?	Summary	Adjusted P-Value	A-M
Control vs. 10	0.98	-5.224 to 7.19	No	ns	>.999	B
Control vs. 50	5.99	-0.2171 to 12.2	No	ns	0.063	C
Control vs. 100	40.90	34.69 to 47.1	Yes	***	<.001	D
Control vs. 150	56.79	50.59 to 63	Yes	***	<.001	E
Control vs. 200	55.59	49.38 to 61.79	Yes	***	<.001	F
Control vs. 250	59.77	53.56 to 65.97	Yes	***	<.001	G
Control vs. 300	63.01	56.8 to 69.21	Yes	***	<.001	H
Control vs. 350	65.89	59.68 to 72.09	Yes	***	<.001	I
Control vs. 400	70.47	64.26 to 76.68	Yes	***	<.001	J
Control vs. 450	74.88	68.67 to 81.08	Yes	***	<.001	K
Control vs. 500	85.17	78.96 to 91.37	Yes	***	<.001	L
Control vs. 70	25.42	19.21 to 31.63	Yes	***	<.001	M

**Table 8:** Statistical analysis of the etoricoxib treatment to the chick embryos. ANOVA followed by Dunnett's multiple test was performed to check the significance of the difference between the percentage survival in each group as compared to control as well as the fitness of the overall test.

Days of Isolation	Activity (nmoles/min/mL)			Activity (nmoles/min/mL)		
	Control			Treated		
	COX-1	COX-2	Total	COX-1	COX-2	Total
1	0.056±0.003	1.915±0.039 <sup>###</sup>	2.009±0.020	0.004±0.002 <sup>***</sup>	0.647±0.009 <sup>***###</sup>	0.671±0.016 <sup>***</sup>
2	0.044±0.001	0.925±0.015 <sup>###</sup>	0.995±0.015	0.295±0.077 <sup>*</sup>	0.277±0.026 <sup>***</sup>	0.577±0.009 <sup>***</sup>
3	0.063±0.002	0.797±0.029 <sup>###</sup>	0.917±0.012	0.068±0.002	0.323±0.032 <sup>***###</sup>	0.489±0.012 <sup>***</sup>
4	0.009±0.005	0.129±0.011 <sup>###</sup>	0.183±0.024	0.002±0.001	0.110±0.008 <sup>###</sup>	0.151±0.002
5	0.011±0.001	0.280±0.007 <sup>###</sup>	0.325±0.017	0.044±0.016	0.143±0.040 <sup>*</sup>	0.240±0.005 <sup>**</sup>
6	0.014±0.003	0.339±0.006 <sup>###</sup>	0.386±0.009	0.180±0.014 <sup>***</sup>	0.086±0.001 <sup>***</sup>	0.280±0.007 <sup>***</sup>
7	0.012±0.004	0.100±0.015 <sup>###</sup>	0.456±0.010	0.013±0.002	0.215±0.022 <sup>*###</sup>	0.287±0.009 <sup>***</sup>
8	0.024±0.002	0.549±0.042 <sup>###</sup>	0.791±0.014	0.025±0.009	0.260±0.006 <sup>*###</sup>	0.299±0.008 <sup>***</sup>
9	0.026±0.004	0.576±0.028 <sup>###</sup>	0.811±0.006	0.143±0.012 <sup>***</sup>	0.140±0.023 <sup>***</sup>	0.304±0.003 <sup>***</sup>
10	0.140±0.108	0.634±0.009 <sup>#</sup>	0.842±0.026	0.251±0.005	0.120±0.009 <sup>***###</sup>	0.378±0.011 <sup>***</sup>

**Table 9:** COX activity assay. Overall, COX activity was significantly depleted by the addition of Etoricoxib. Diminution of total COX activity was due to reduced COX-2 activity since COX-1 activity remained close to nil in control embryos and rose in some treated embryos when COX-2 activity was curtailed. The activity of COX-1 reached close to that of COX-2 in days 2, 6, and 9 of the treatment group, whereas control embryos at this stage showed a significant difference between COX-1 and COX-2 activities. Day-4 embryos showed thorough compensation of allayed COX-2 activity by COX-1, and thus total activity became non-significant in comparison with control group total activity. Significance values derived by comparing the activity of the treatment group with the respective activity of the control group are expressed as Mean ± SEM; \* $p \leq 0.05$ , \*\* $p \leq 0.01$ , \*\*\* $p \leq 0.001$ ,  $n=3$ . Differences between COX-1 and COX-2 activities are expressed here as Mean ± SEM; # $p \leq 0.05$ , ## $p \leq 0.01$ , ### $p \leq 0.001$ ,  $n=3$ .

Day	COX-1		COX-2	
	Mean Cq	Initial copy numbers	Mean Cq	Initial copy numbers
1	26.51	2254.907	24.27	2890.351
2	26.82	2225.776	24.77	2642.857
3	27.71	2172.259	25.12	2518.508
4	27.67	2173.958	25.70	2373.885
5	27.51	2181.301	25.77	2360.418
6	27.34	2190.165	25.88	2340.675
7	28.40	2149.903	26.70	2236.233
8	26.96	2214.741	25.21	2491.608
9	31.54	2120.971	22.53	5081.143
10	26.98	2213.260	25.25	2480.241

**Table 10:** Absolute quantity of COX-1 and COX-2 transcripts in control chick embryos. The initial numbers were derived from the standard graph using a non-linear fit analysis tool of GraphPad Prism.

Days of Isolation	COX-1 band intensity	COX-2 band intensity	GAPDH band intensity	Relative Band Intensity (COX-1/GAPDH)	COX-1 protein level	Relative Band Intensity (COX-2/GAPDH)	COX-2 protein level
1	85.896	172.374	055.213	1.556	155.572	3.122	312.198
2	82.716	164.518	099.553	0.831	083.087	1.653	165.257
3	79.871	085.432	121.921	0.655	065.510	0.701	070.072
4	76.436	080.491	174.676	0.438	043.759	0.461	046.080
5	81.087	100.817	187.555	0.432	043.234	0.538	053.753
6	81.757	111.756	186.548	0.438	043.826	0.599	059.907
7	84.648	137.459	192.555	0.440	043.960	0.714	071.387
8	81.278	138.257	200.370	0.406	040.564	0.690	069.001
9	80.705	155.431	190.064	0.425	042.462	0.818	081.778
10	84.348	150.658	171.853	0.491	049.081	0.877	087.667

**Table 11:** Densitometric analysis of COX-1, COX-2, and GAPDH blots. The values were derived using grey-scale densitometric analysis in doc-ItLs software. The calculated relative band intensities (converted into percentage) were plotted in figure 17. The mean values of COX-1 protein and COX-2 protein concentrations were significantly different than each other, as shown in the two-way ANOVA table below.

<b>ANOVA table</b>	<b>SS</b>	<b>DF</b>	<b>MS</b>	<b>F (DFn, DFd)</b>	<b>P-value</b>
<b>Interaction</b>	29756	9	3306	F (9, 40) = 43.01	P<.001
<b>Row Factor</b>	182475	9	20275	F (9, 40) = 263.8	P<.001
<b>Column Factor</b>	24234	1	24234	F (1, 40) = 315.3	P<.001
<b>Residual</b>	3075	40	76.87		
<b>Source of Variation</b>	% of the total variation		P-value	P-value summary	Significant?
<b>Interaction</b>	12.42		<.001	***	Yes
<b>Row Factor</b>	76.18		<.001	***	Yes
<b>Column Factor</b>	10.12		<.001	***	Yes

*Table 12: ANOVA of COX blots showing significantly varied concentration of these isoenzymes*

## FIGURES

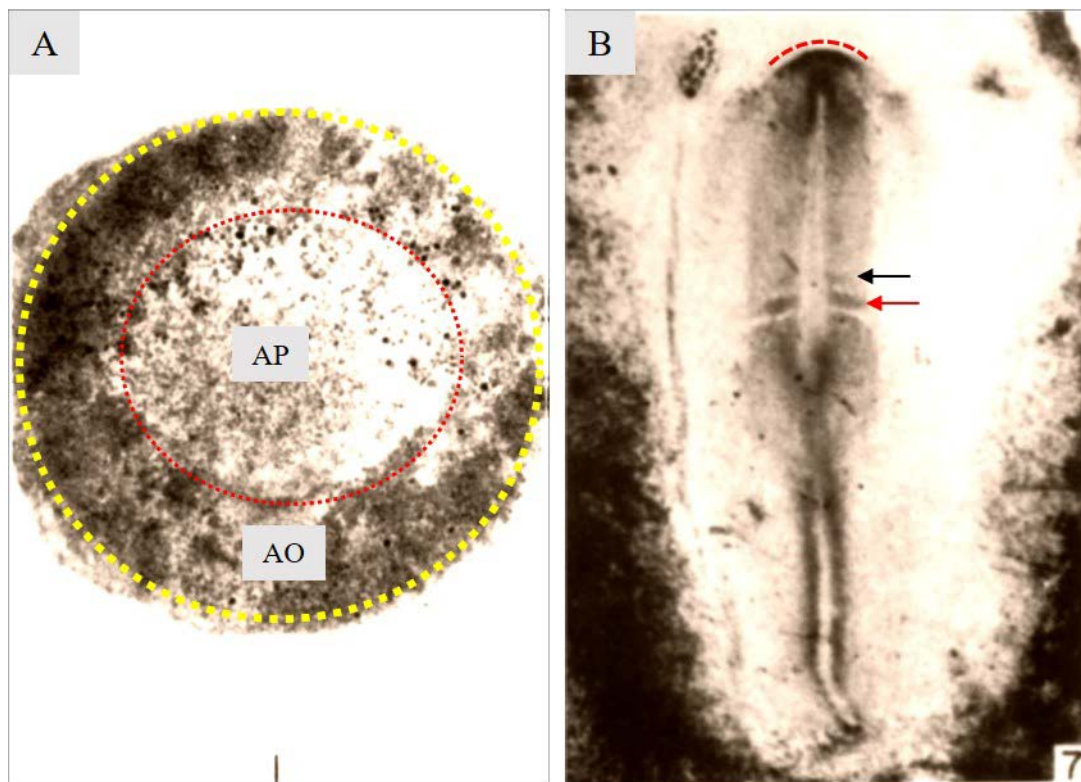


**Figure 5:** Morphology of chick embryo on day-0 (A) and day-1 (B). A: Boundary of Area Pellucida (AP) is shown with the help of red dotted line and that of Area Opaca (AO) with yellow dotted line. Day-0 embryo is HH 1 stage. B: first under-developed somite shown with black arrow and second fully developed somite with red arrow. The head-fold is shown using red interrupted curve-line here. Day-1 embryo is HH 6 and HH 7 both, which contain some common characteristics as described in table 2. (derived from Hamburger-Hamilton, 1951).

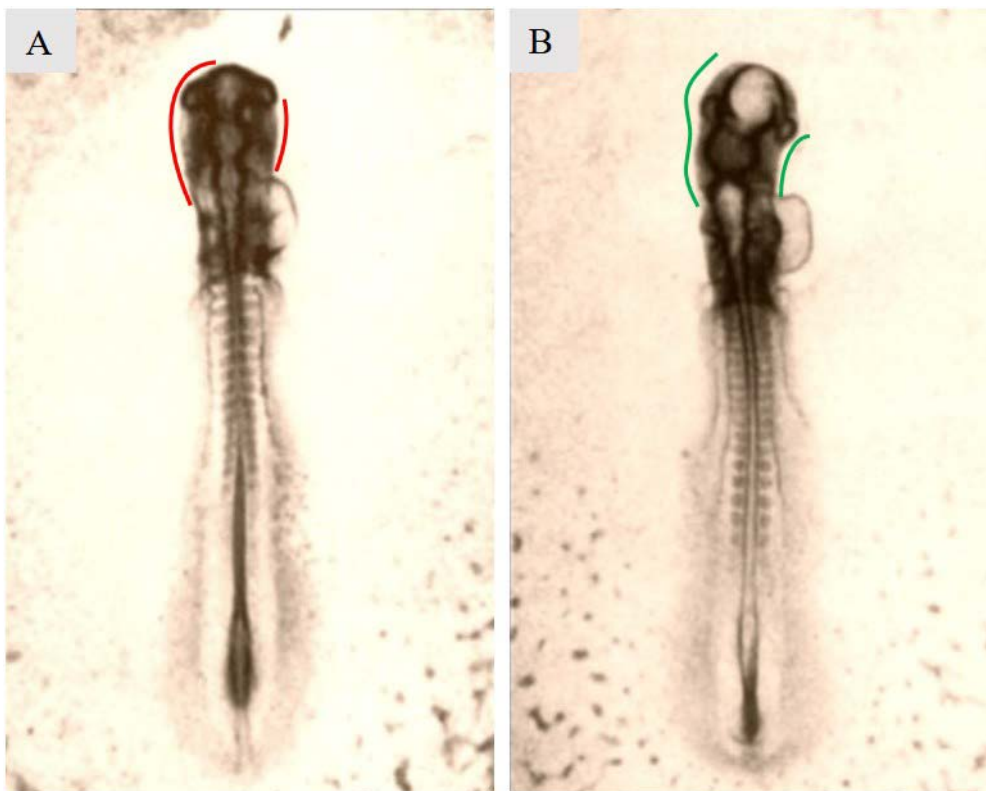


**Figure 6:** Morphology of chick embryo on day-2. A: HH 12 (16 somites, 45-49 hours). The embryo is straight. Optic vesicles are present. The upper body shape not showing curvature is shown with the help of red lines. B: HH 13 (19 somites, 48-52 hours). The embryo starts to show the signs of flexure at the upper body. The curvature is shown with the help of green lines. (derived from Hamburger-Hamilton, 1951).

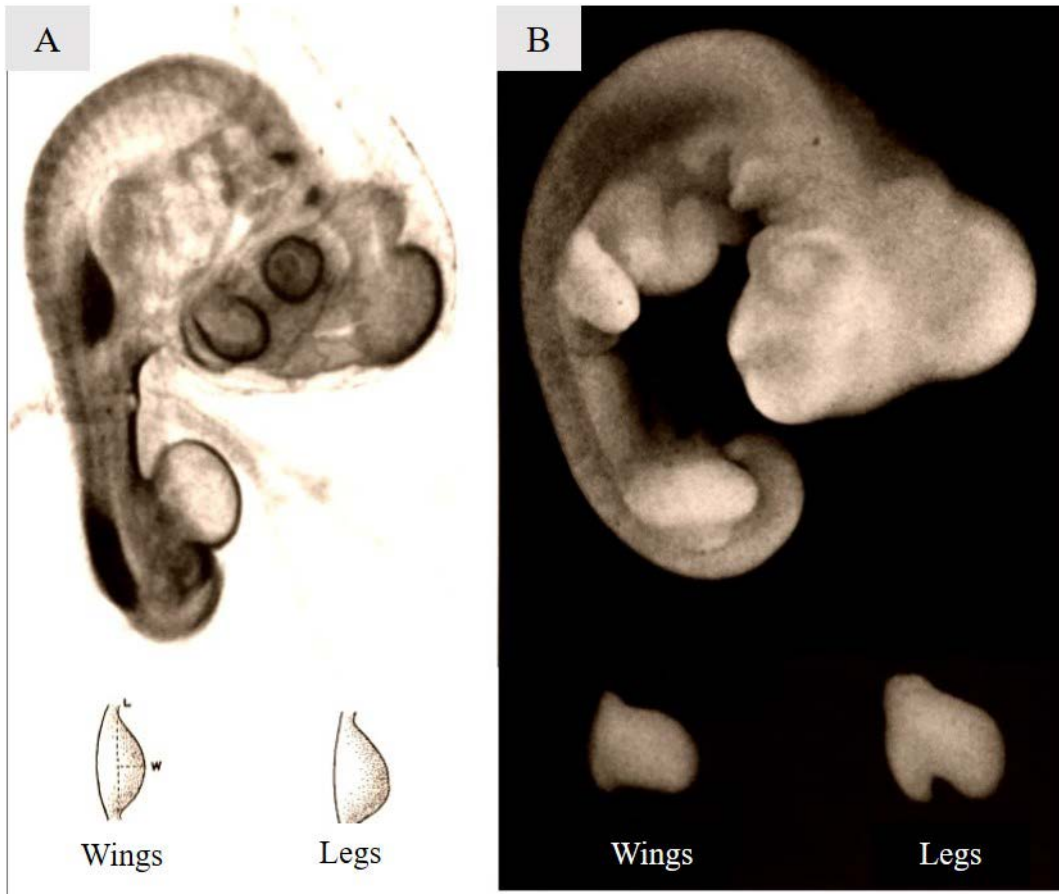


**Figure 7:** Morphology of chick embryo on day-3 (A) and day-4 (B). A: A three-day old embryo, with little grown limb buds. B: four-day old embryo with considerably long limbs, no longer to be called as 'buds'. (derived from Hamburger-Hamilton, 1951).

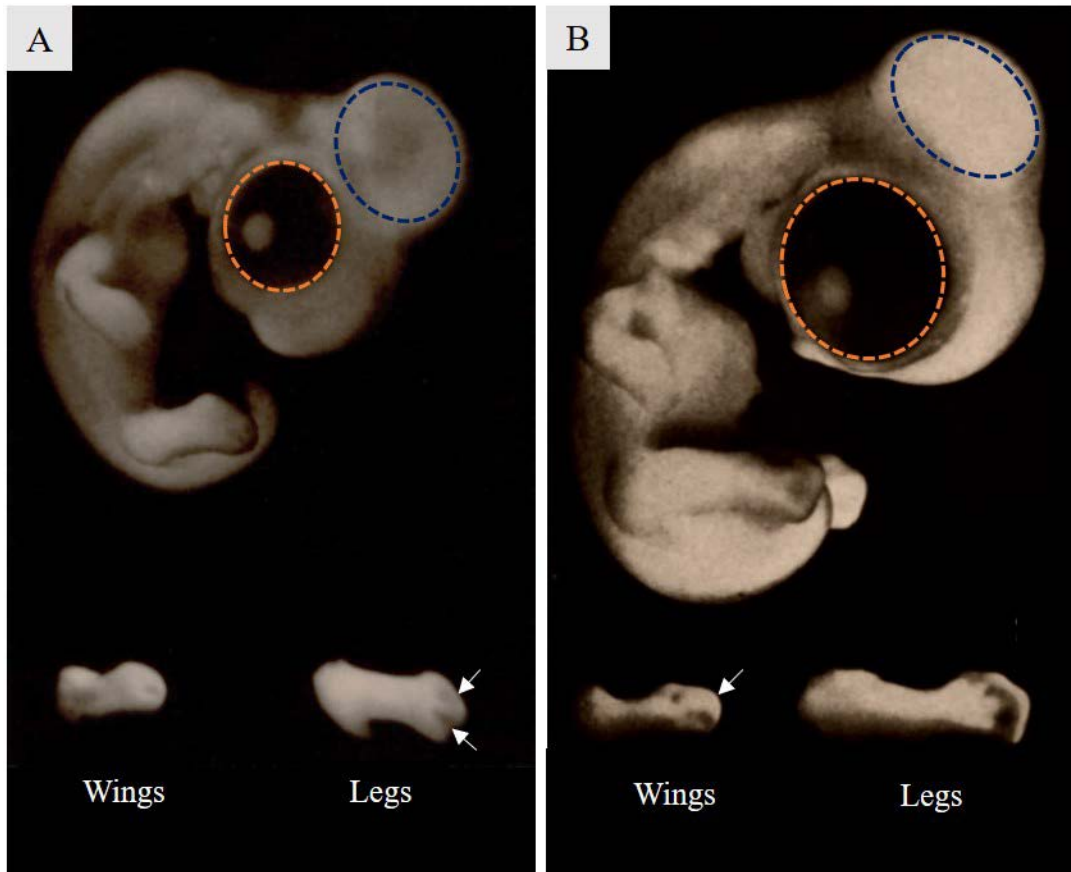


**Figure 8:** Morphology of chick embryo on day-5 (A) and day-6 (B). A: first, second, and third toes (digits in hindlimb) look internally separated by a groove (shown with the help of white arrows). Eyes (orange dotted circle) are smaller or equal in size to the forebrain lobe (blue dotted circle) B: second forelimb digit is longer than all other forelimb digits (shown with white arrow). Eyes (orange dotted circle) are visibly larger than the forebrain lobe (blue dotted circle). (derived from Hamburger-Hamilton, 1951).

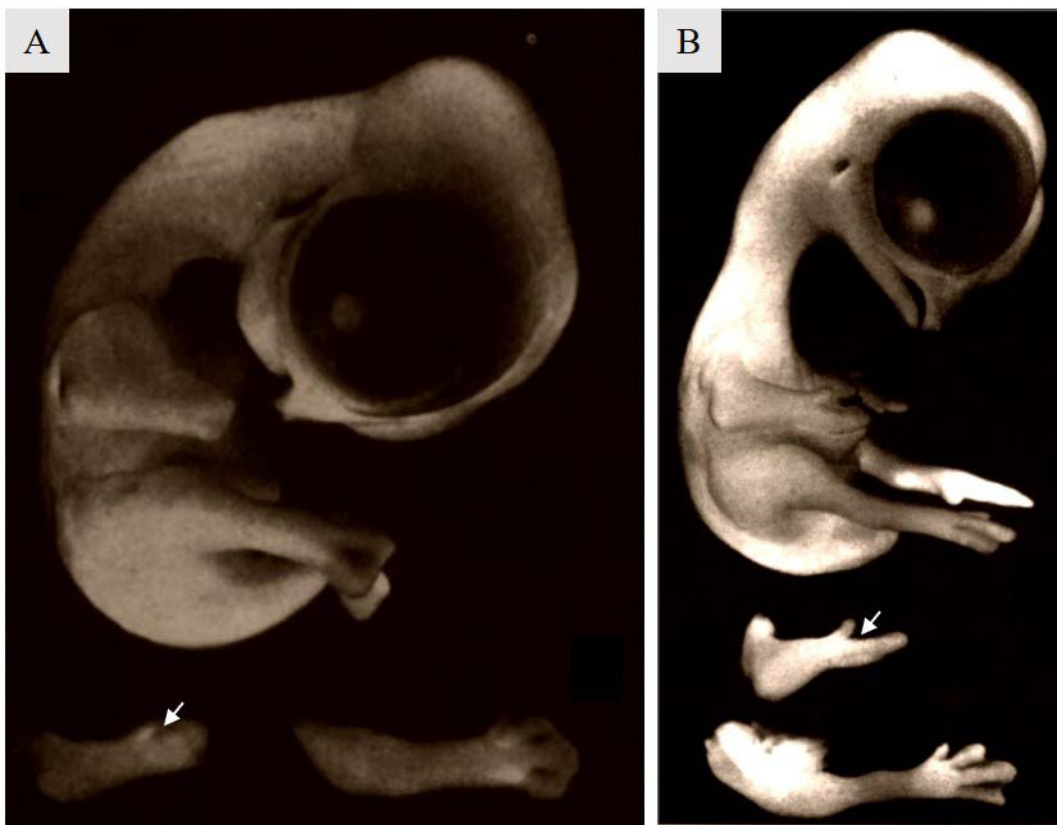


**Figure 9:** Morphology of chick embryo on day-7 (A) and day-8 (B). A: First and second digits of forelimb are attached by thin web (shown with the help of white arrow). B: First and second digits of forelimb are free from each other. The membranous web present between these are digested. (derived from Hamburger-Hamilton, 1951).

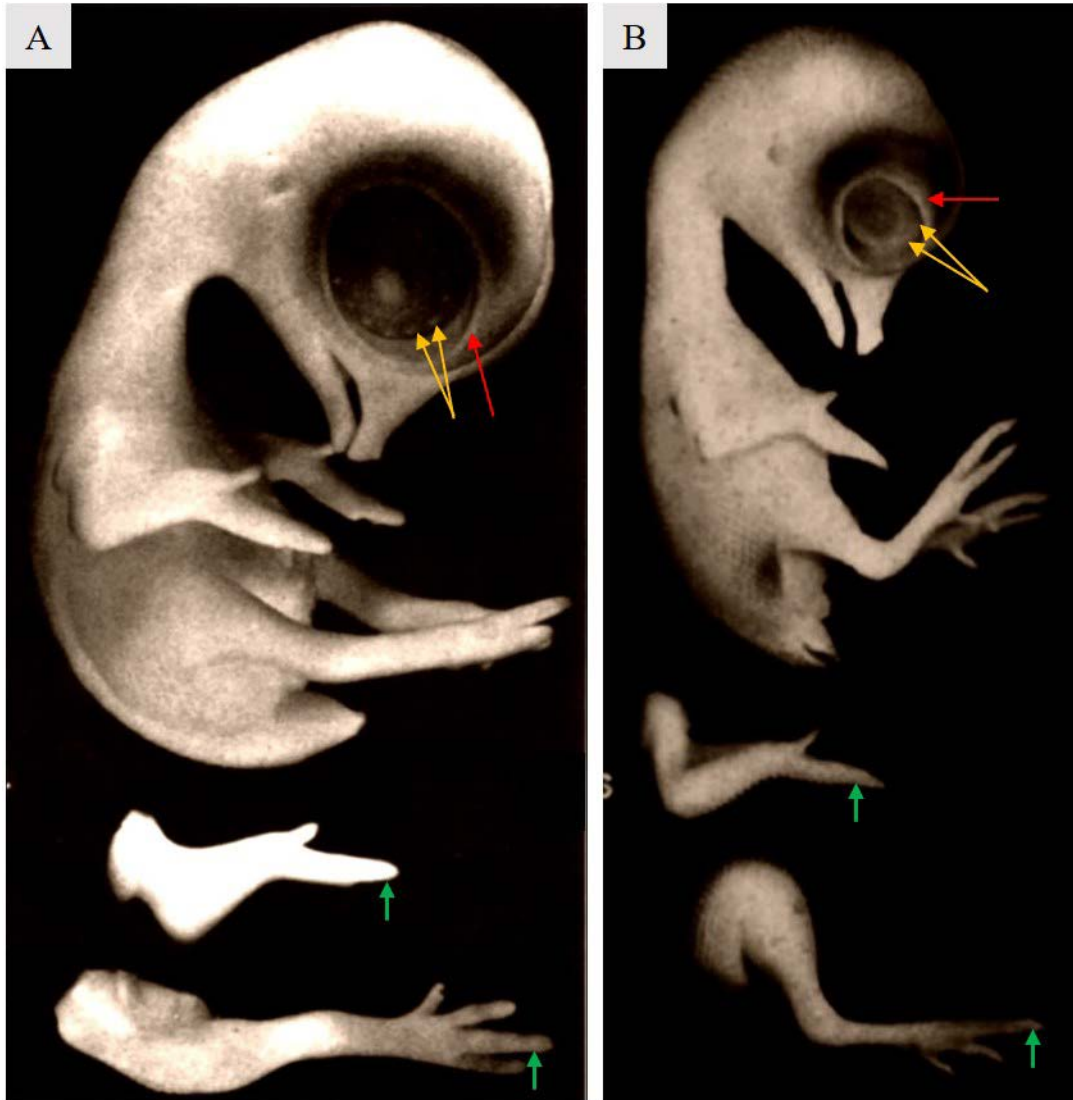


**Figure 10:** Morphology of chick embryo on day-9 (A) and day-10 (B). A: The nictitating membrane (red arrow) starts to migrate towards the scleral papillae (yellow arrows). Limbs have smaller digits (green arrows) lacking the distal curvature as seen in the next stage. This stage (HH 35 is actually not day-9, rather is day-8/9, showing overlapping timepoints between stages). B: Nictitating membrane (red arrow) reaches the scleral papillae (yellow arrows). Limbs have extensively grown digits showing a typical curvature at their distal ends (green arrows). All the components of hindlimbs are visibly longer than that on day-9. (derived from Hamburger-Hamilton, 1951).



**Figure 11:** Morphology of chick embryo on day-11 (A) and day-12 (B). The only visibly obvious difference is that the nictitating membrane almost closes on day-12 as compared to day-11. The gap between the membrane edges is shown with the help of red line in day-11 (A) and with green line in day-12 (B). (derived from Hamburger-Hamilton, 1951).

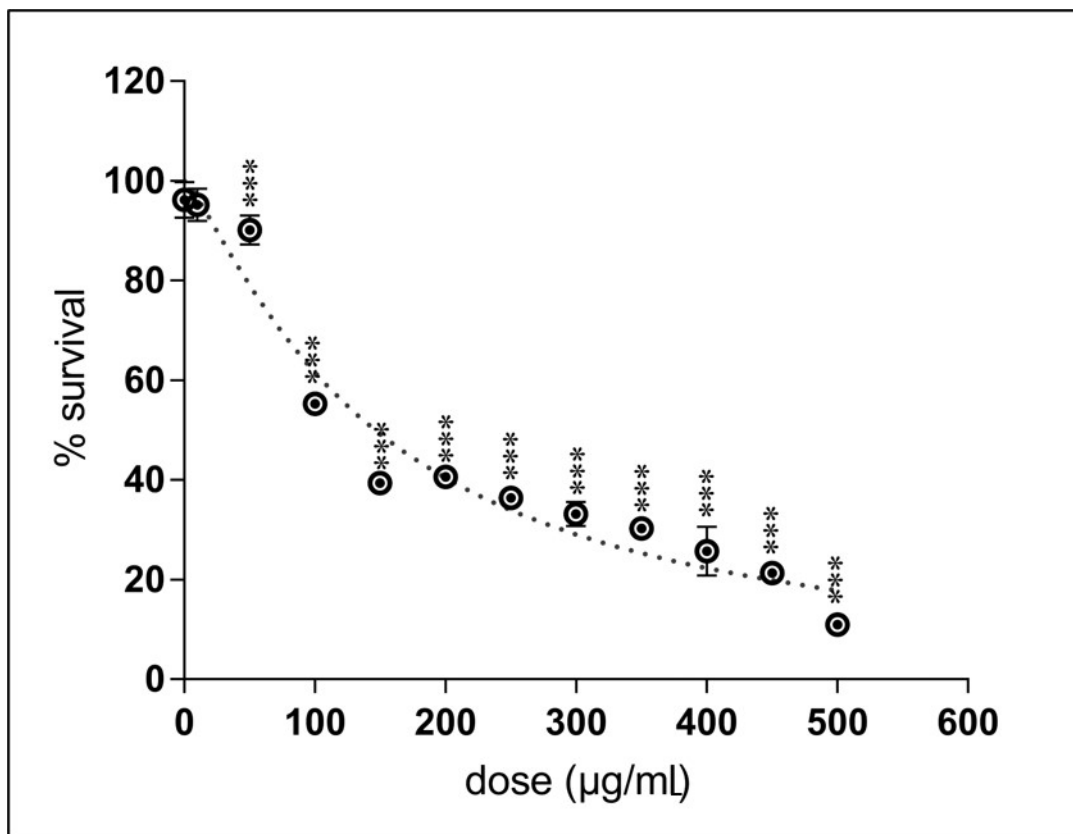


**Figure 12:** Dose range analysis of etoricoxib in chick embryos. Survival of embryos decreased when treatment concentration was increased. Less than 20 % embryos survived when 500 µg/mL concentration of etoricoxib was administered. Plotted values are mean ± SEM. Significance values were derived using ANOVA followed by Dunette's multiple t-tests. The mean survival rates of all groups were compared with that of the control group. \*\*\*p value < 0.001. n = 30 for control group and n = 50 for treatment group.

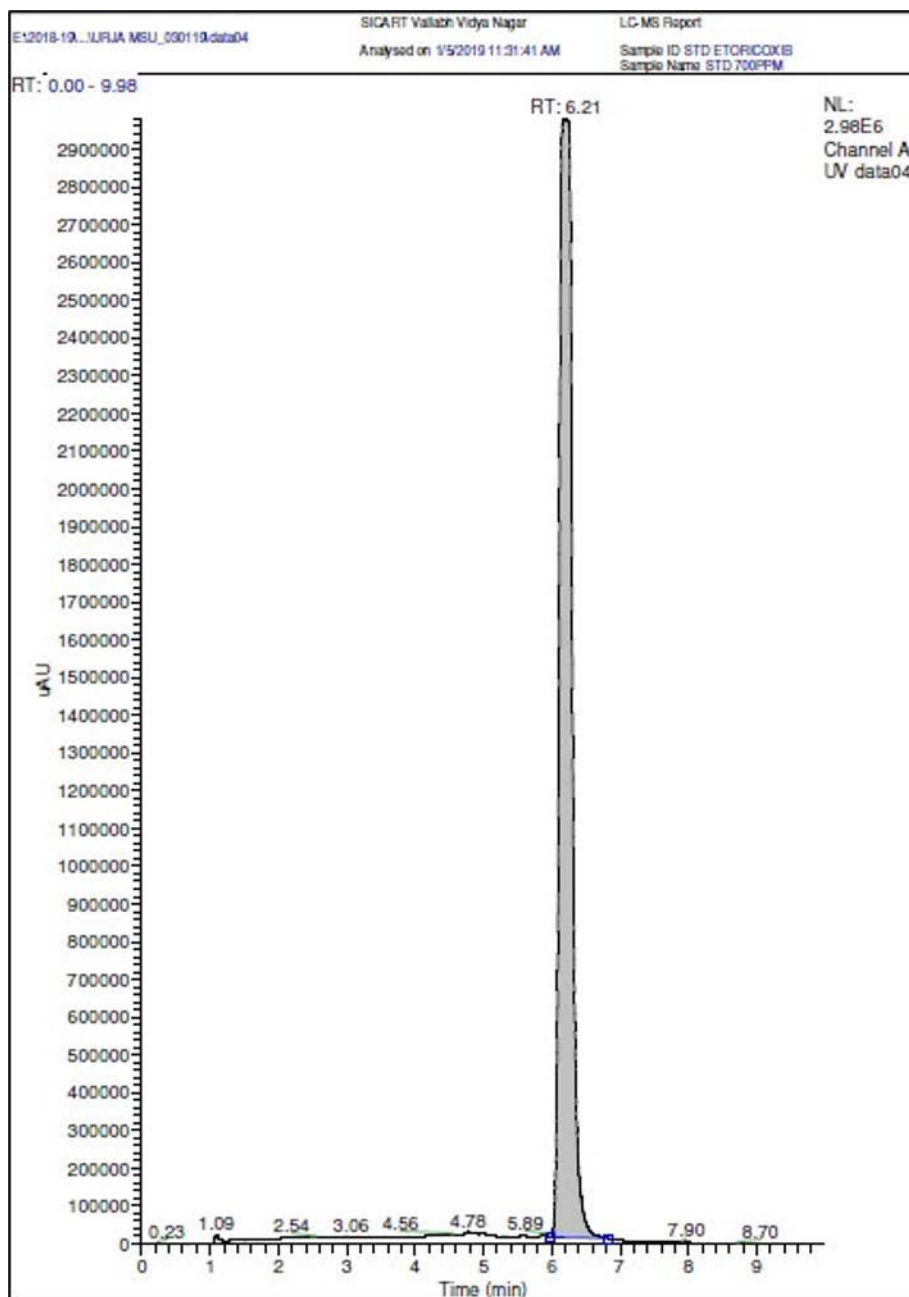


**Figure 13A:** Liquid chromatography profile of standard solution of etoricoxib. The only peak present appeared at 6.21 minutes. The grey highlighted area was magnified to see the mass peak of chemicals eluting at that point of time. Unit of Y-axis: mAU: milli absorbance unit.

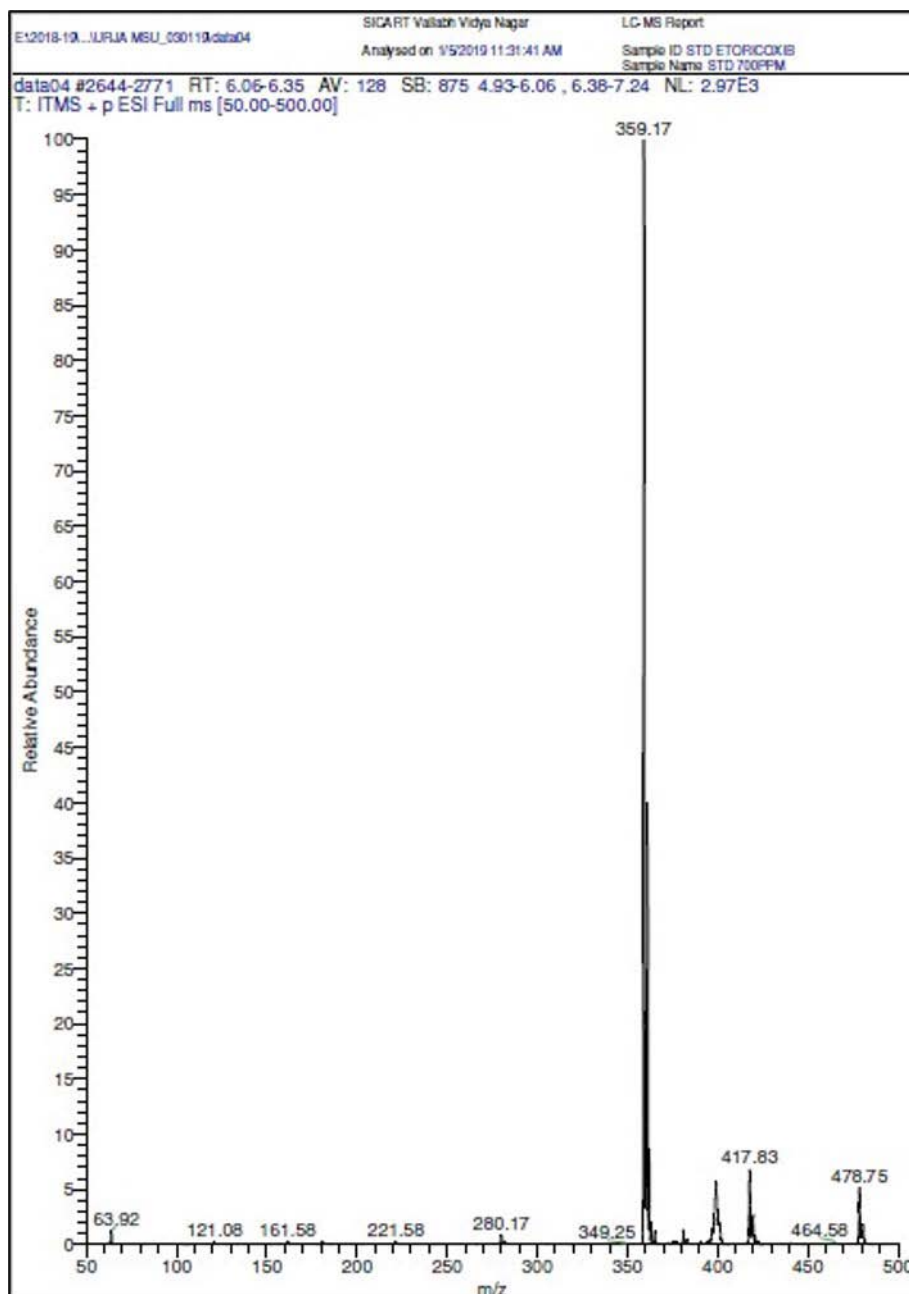


**Figure 13B:** Mass spectrum of compounds eluting within the highlighted area in figure 13A. A peak of 359 visible here is a mass peak appearing in positive mode for etoricoxib, as its molecular weight is 358. This is a standard solution containing negligible amount of impurities. Therefore, the visible peak is of etoricoxib only.  $m/z$  on X-axis stands for mass to charge ratio.

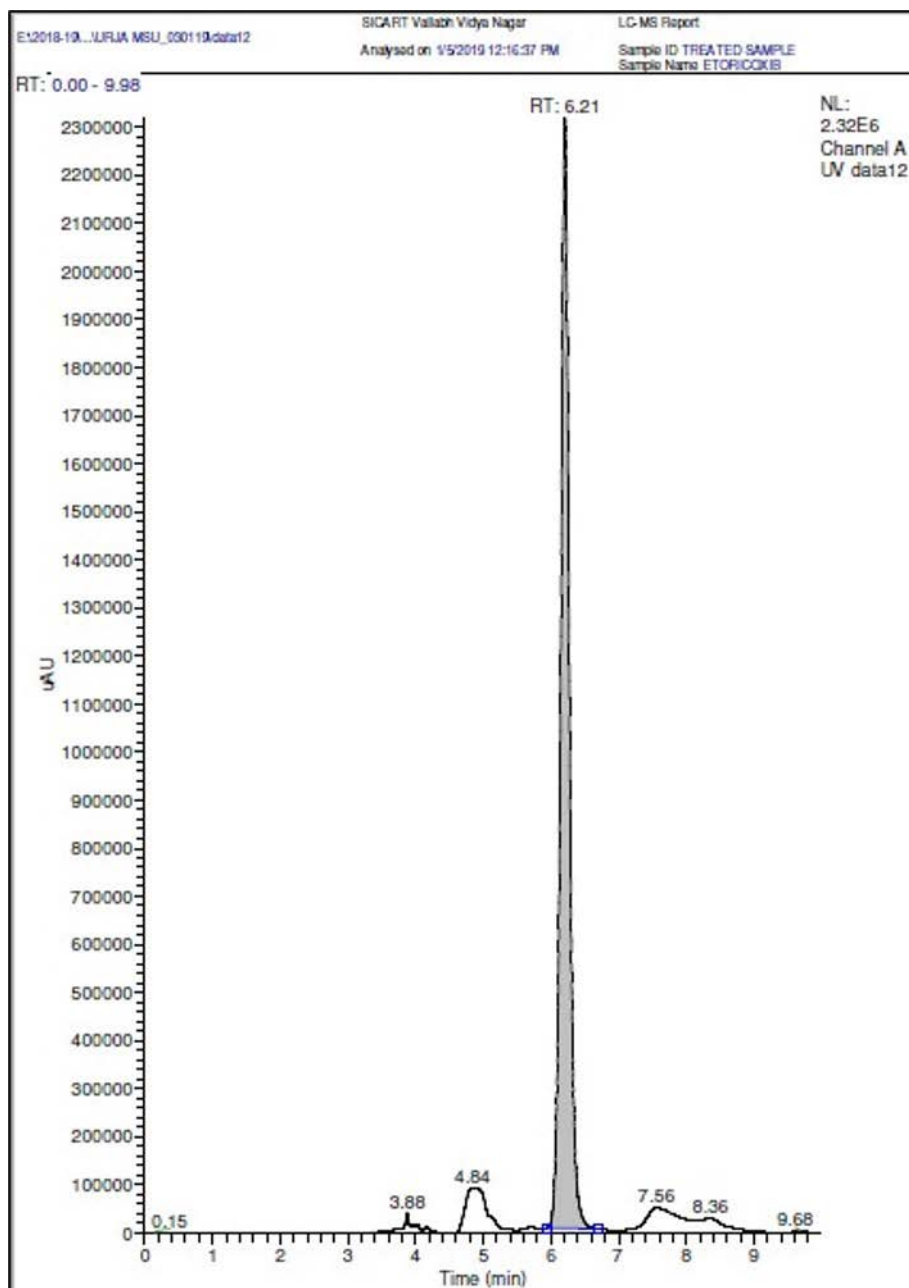


**Figure 13C:** Liquid chromatography profile of experimental group embryos. The day-2 embryonic sample showed largest peak at 6.21 minutes. The grey highlighted area was magnified to see the mass peaks of chemicals eluting at that point of time. Unit of Y-axis: mAU: milli absorbance unit.

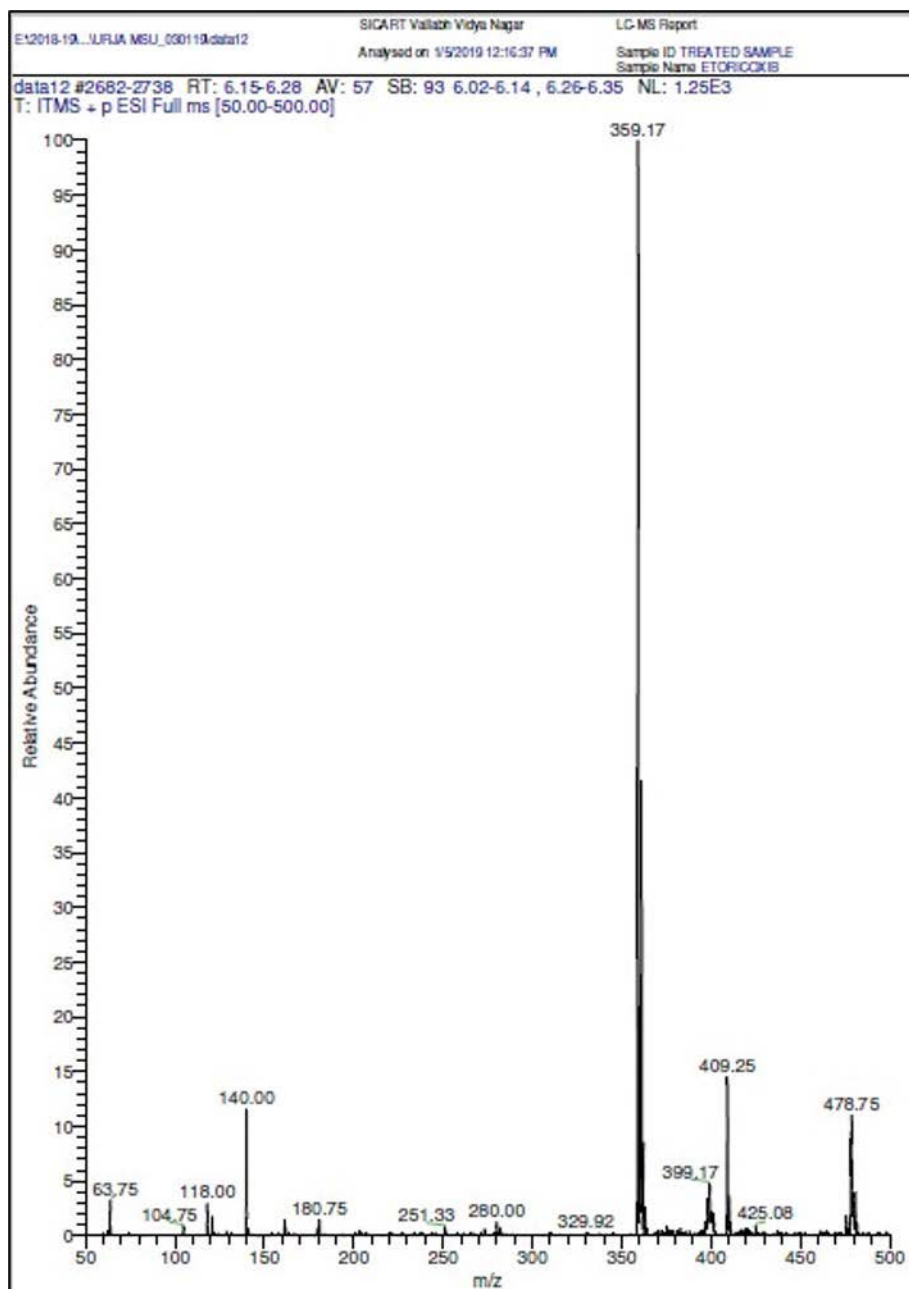


**Figure 13D:** Mass spectrum of compounds eluting within the highlighted area in figure 13C. A peak of 359 visible here is a mass peak appearing in positive mode for etoricoxib, as its molecular weight is 358.  $m/z$  on X-axis stands for mass to charge ratio.

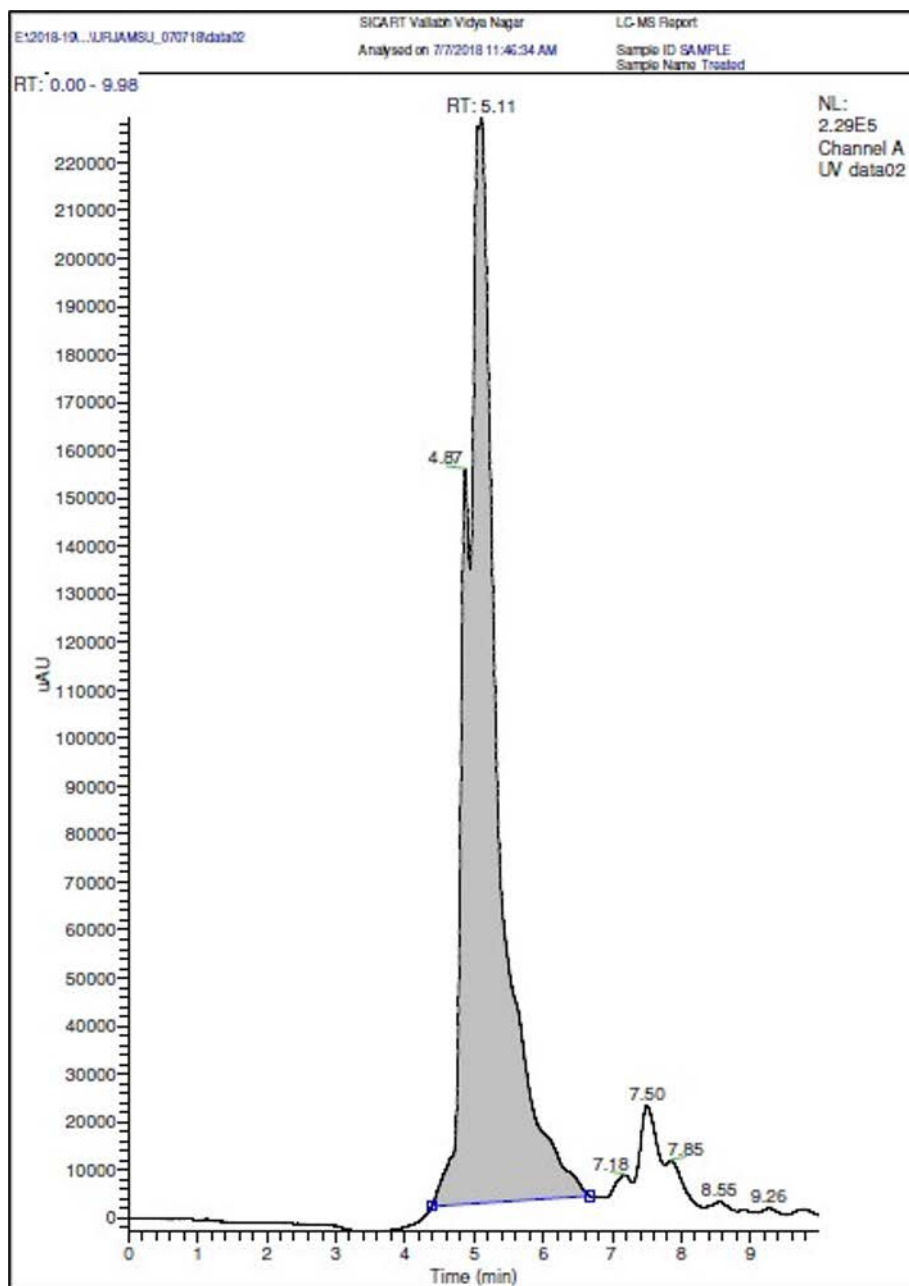


**Figure 13E:** Liquid chromatography profile of embryos belonging to control group. The only peak present appeared between 4 to 7 minutes. The grey highlighted area was magnified to see the mass peak of chemicals eluting at that point of time. Unit of Y-axis: mAU: milli absorbance unit.

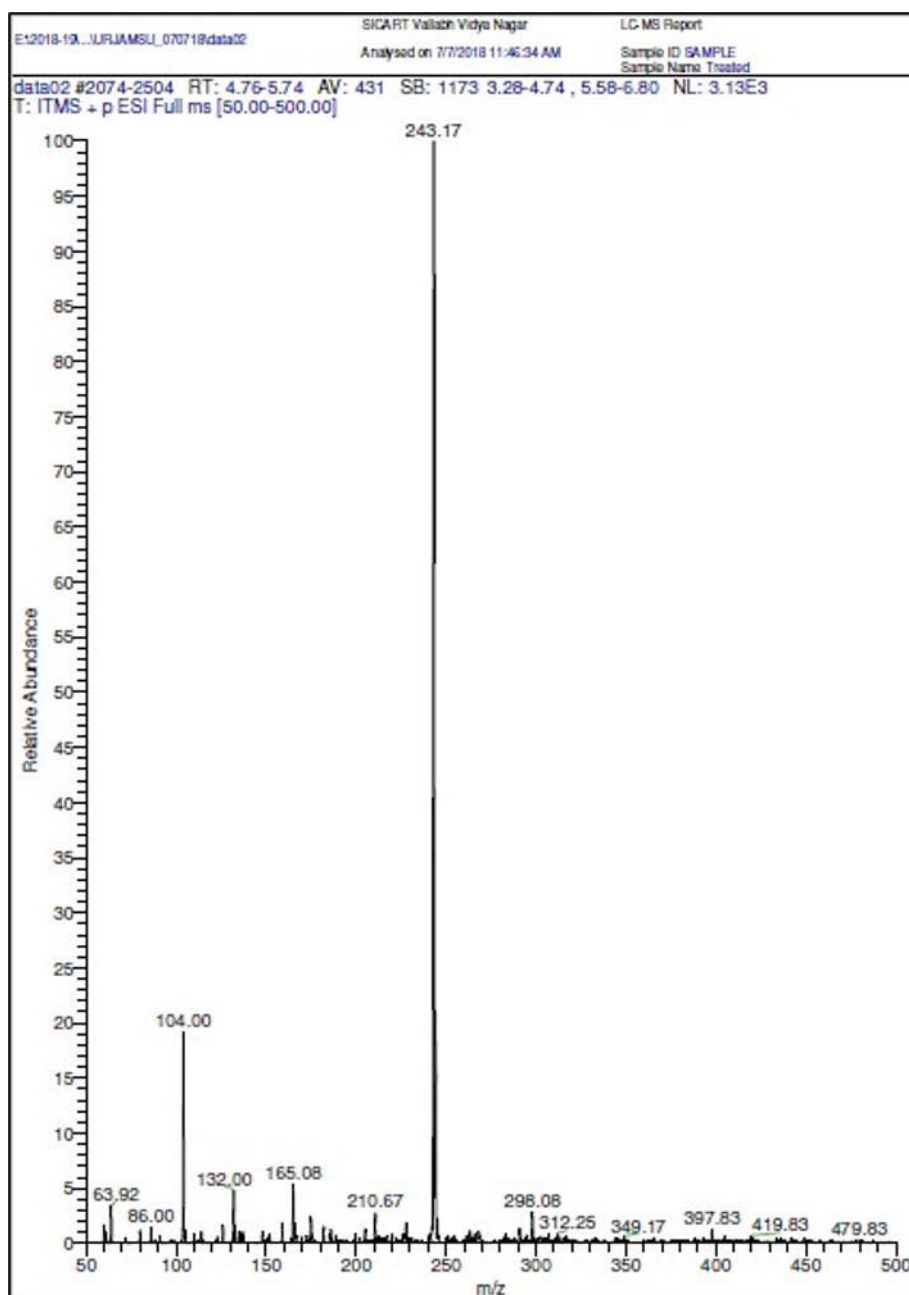


**Figure 13F:** Mass spectrum of compounds eluting within the highlighted area in figure 13E. A peak of 243 visible here is not a mass peak appearing in positive mode for etoricoxib in its standard solution. The relative abundance as plotted on Y axis showed that the peak present between 4 to 7 minutes had extremely low intensity as compared to etoricoxib peak intensity in treated embryos. The peak did not correspond to etoricoxib conclusively.  $m/z$  on X-axis stands for mass to charge ratio.

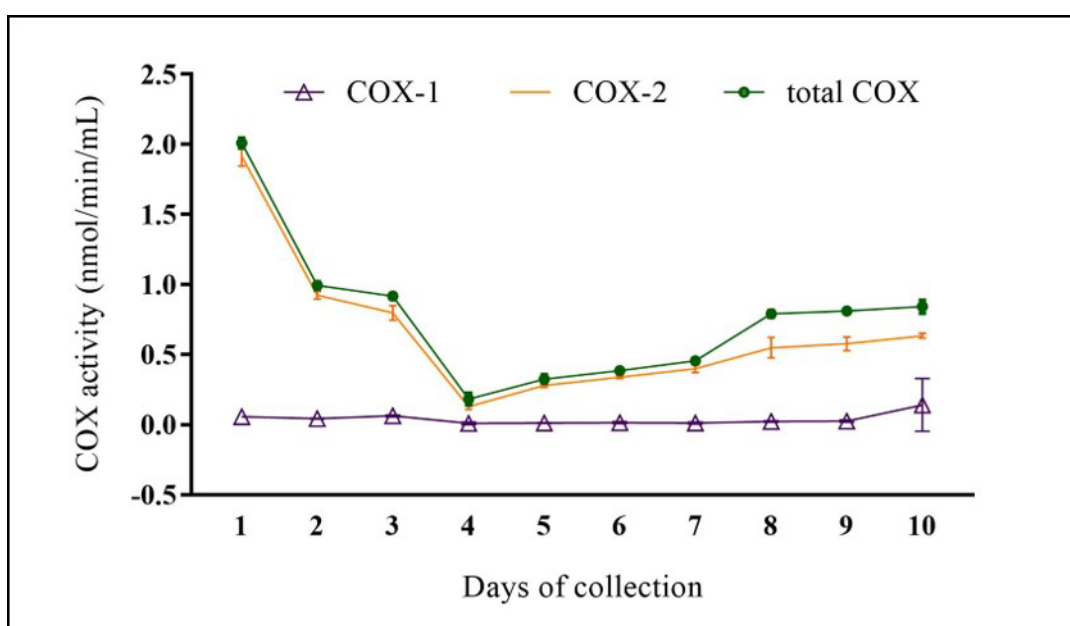


**Figure 14A:** Control COX activity profile. Total COX activity diminished after being highest on day-1. It was least active on day-4 after which it kept increasing slowly till day-7. day-8, day-9, and day-10 embryos showed more or less similar level of COX activity. The trend of total COX activity was followed by COX-2 while COX-1 remained almost inactive showing negligible amount of activity per minute per mL homogenate sample of control embryos. The plotted values are mean  $\pm$  SEM.

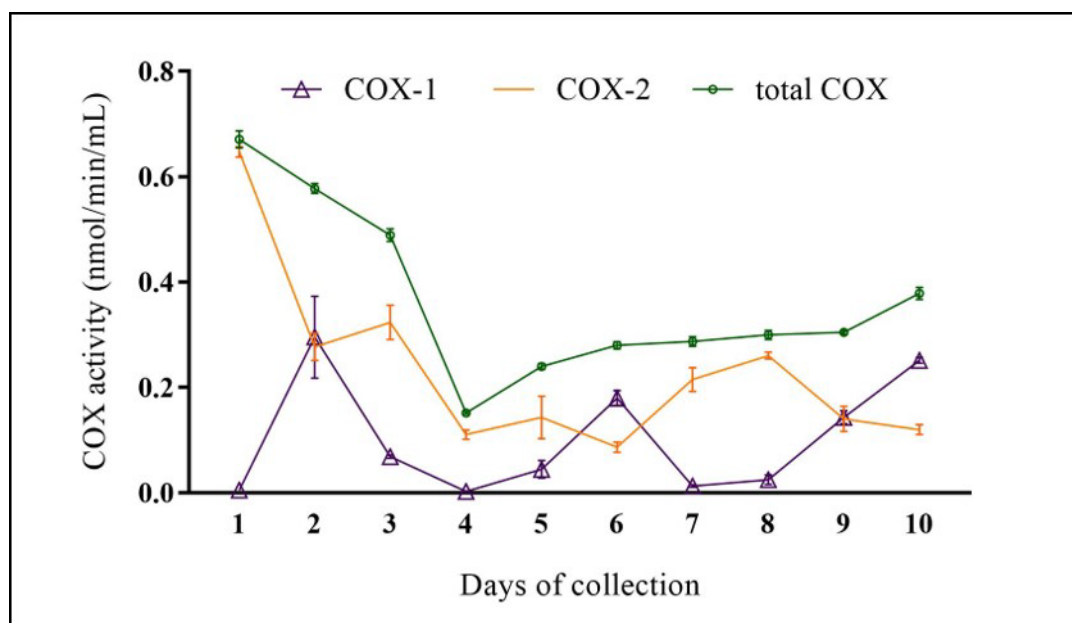


**Figure 14B:** Experimental COX activity profile. Total COX activity diminished after being highest on day-1, but the drop being smaller as compared to that in control group (shown in figure 14A). It was least active on day-4 after which it kept increasing slowly till day-6. day-6 to day-9 embryos showed more or less similar level of COX activity. A small hike was visible on day-10. COX-2 activity did not show similar trend to that of total COX activity. COX-1 activity periodically rose in some stages when COX-2 activity drastically went down. The plotted values are mean  $\pm$  SEM.

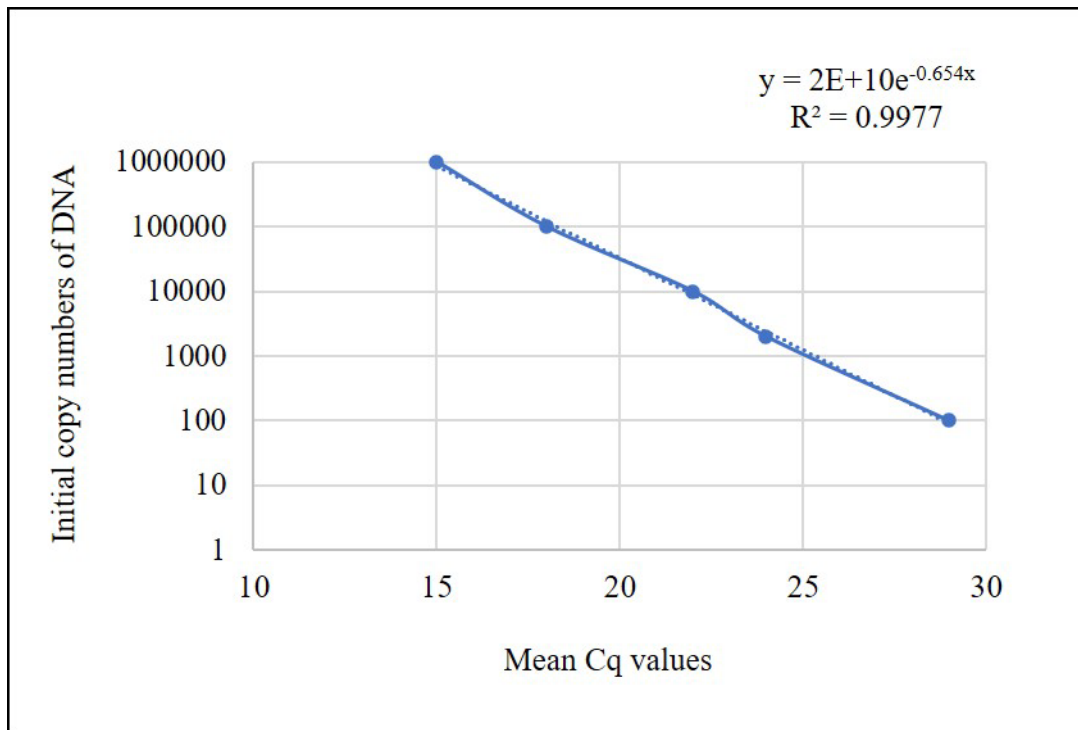


**Figure 15:** Standard graph of qRT-PCR.

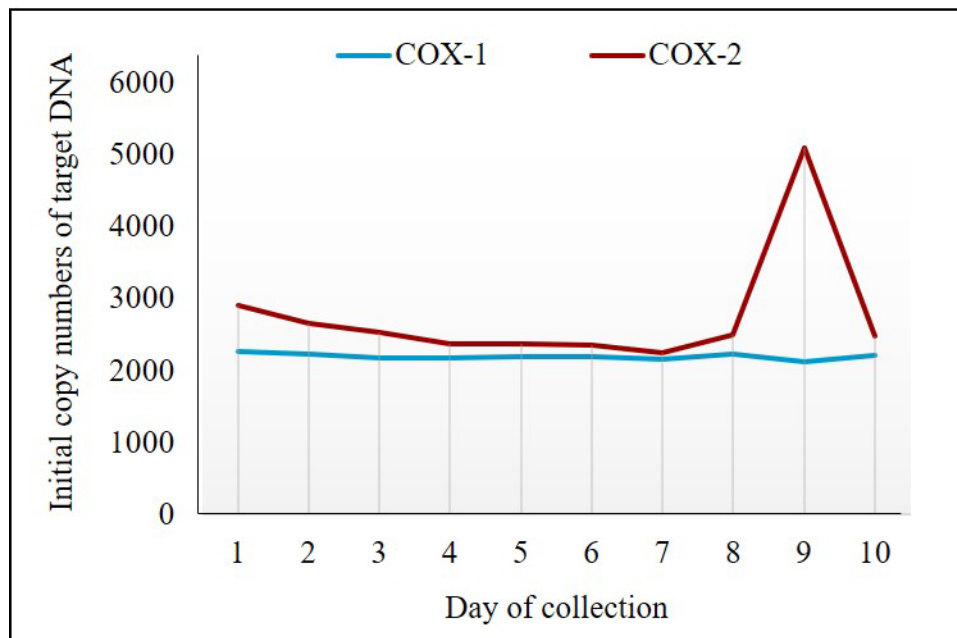


**Figure 16:** qRT-PCR of COX isozymes in control chicks. The copy numbers of COX-1 remained more or less constant throughout from day-1 to day-10. COX-2 transcripts increased only on day-9, which otherwise remained at similar levels to COX-1.

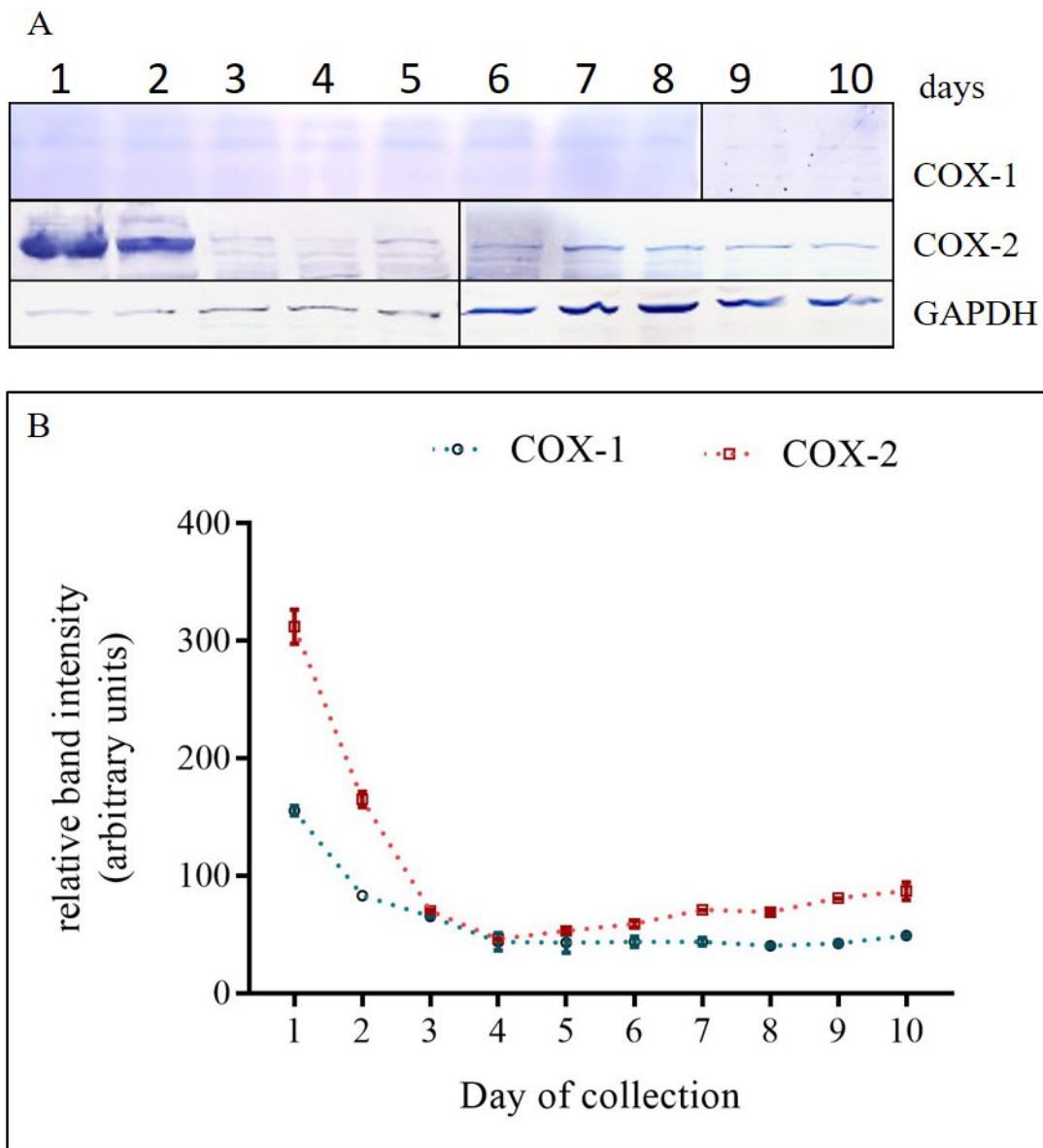


**Figure 17:** Western blot of COX-1 and COX-2. A: Blot images of COX-1, COX-2, and GAPDH blots. COX-1 remained almost undetectable in the samples except for in day-1 and day-2 embryos. COX-2 was higher than COX-1 at almost all the stages. COX-2 peaked at day-1 and decreased till day-4, after which it increased again. The plotted values are mean  $\pm$  SEM from three technical replicates each using three biological replicates.

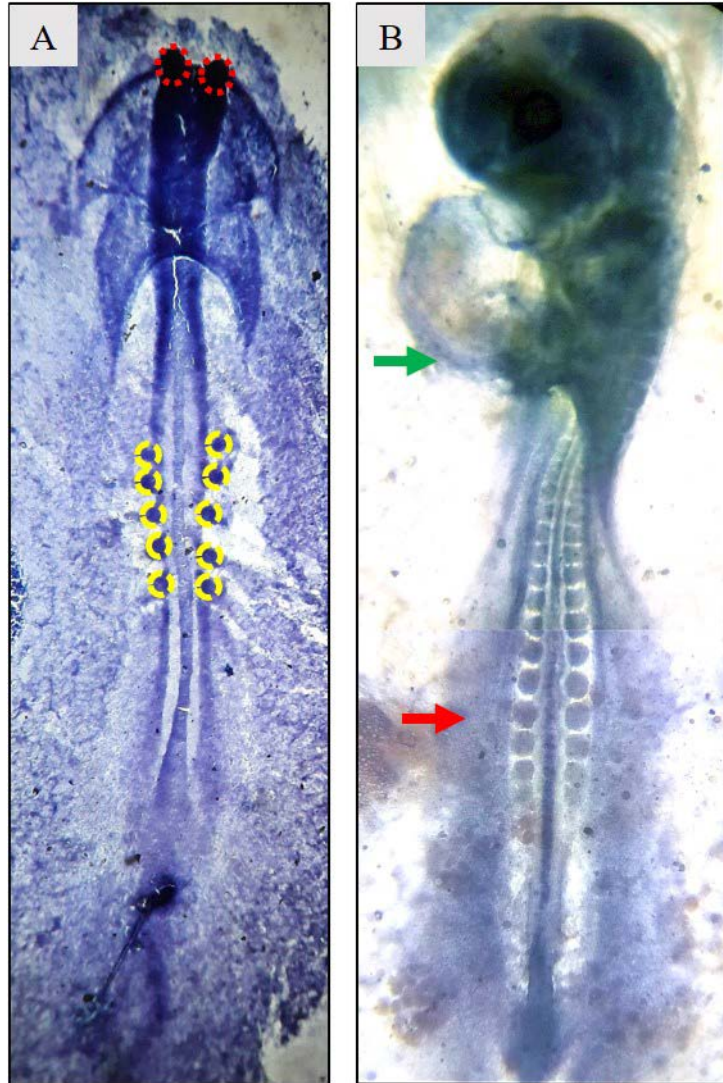


**Figure 18:** Whole mount immunostaining of COX-2 in day-1 (A) and day-2 (B) embryos. A: day-1 embryos showed immunostaining diffused in whole embryo. The darkest stained regions included optic vesicles (circled red), and somites (highlighted with yellow). B: COX-2 localized in more specific areas in day-2 embryos. These especially included heart tube (green arrow) and around somites (red arrow).



**Figure 19:** Immunohistochemistry of COX-2 in day-3 embryo (A) and day-4 embryonic heart (B). A: COX-2 was majorly localized in head (denoted by h), eyes (shown with red arrow), and allantoic vesicle (denoted by av) in day-3 embryo. B: localization of COX-2 in heart tissue in day-4. Both atria (a) and ventricles (v) were stained with COX-2 in diffused manner. Their walls also showed considerable intensity of it (black arrows).

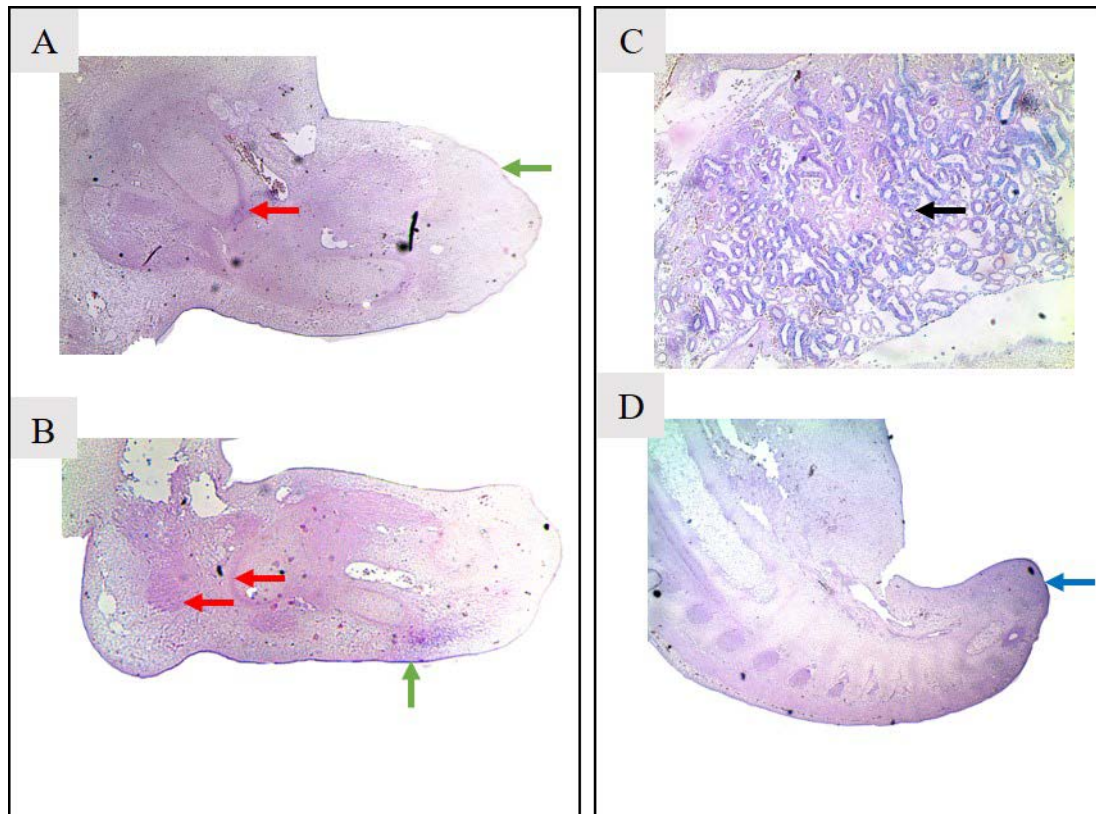


**Figure 20:** Immunolocalization of COX-2 in limbs of day-5 embryos (A and B) as well as kidney of day-7 (C) and lower half of day-8 embryo (D). A: COX-2 localized around the growing bones at the areas of cartilage condensation (red arrows) as well as in the epithelium (green arrow) in the forelimb. B: Presence of COX-2 in the areas of cartilage condensation (red arrows) and epithelium (green arrow) in hindlimb of day-5 embryo. C: Kidney cells of day-6 immunostained by COX-2 antibody (black arrow). D: Tail tip along with somites localized with COX-2 in day-7 embryo (blue arrow).

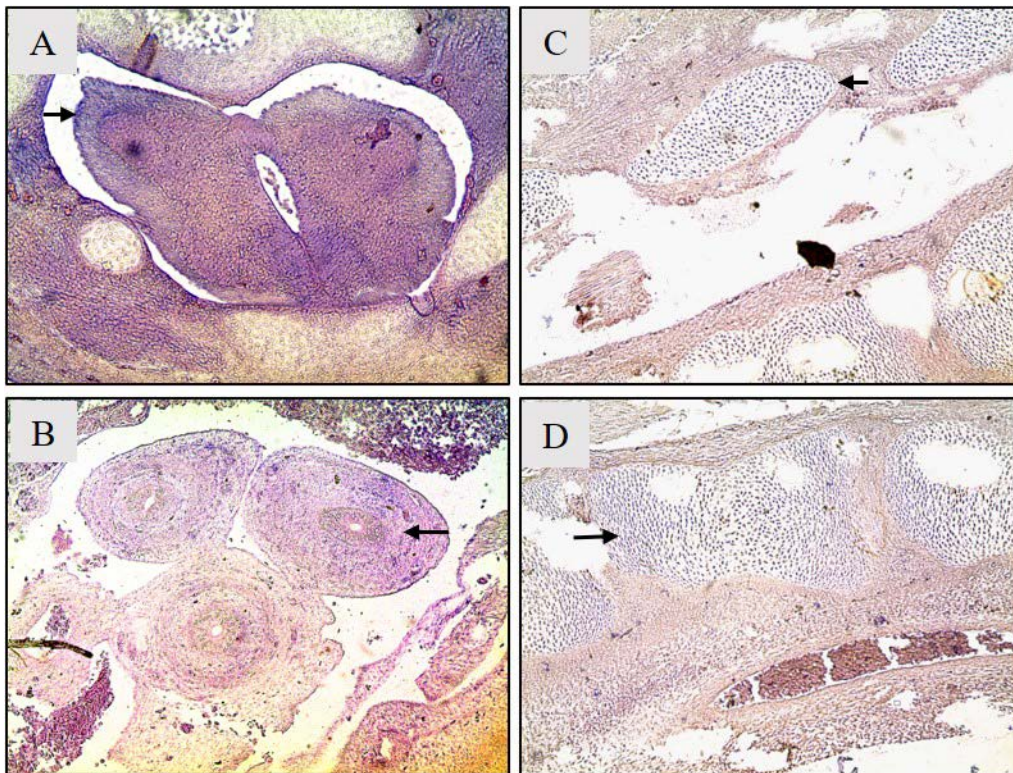


**Figure 21:** COX-2 immunohistochemistry in notochord of day-7 (A), testis of day-8 (B), developing nerve cord (C) and somites (D) at day-9. A: Transverse section through day-7 embryonic developing notochord. B: Seminiferous vesicle of growing testis stained by COX-2 antibody. C: Nerve cord of day-9 stained with COX-2 antibody (black arrow). D: COX-2 immunolocalized in day-9 somites.

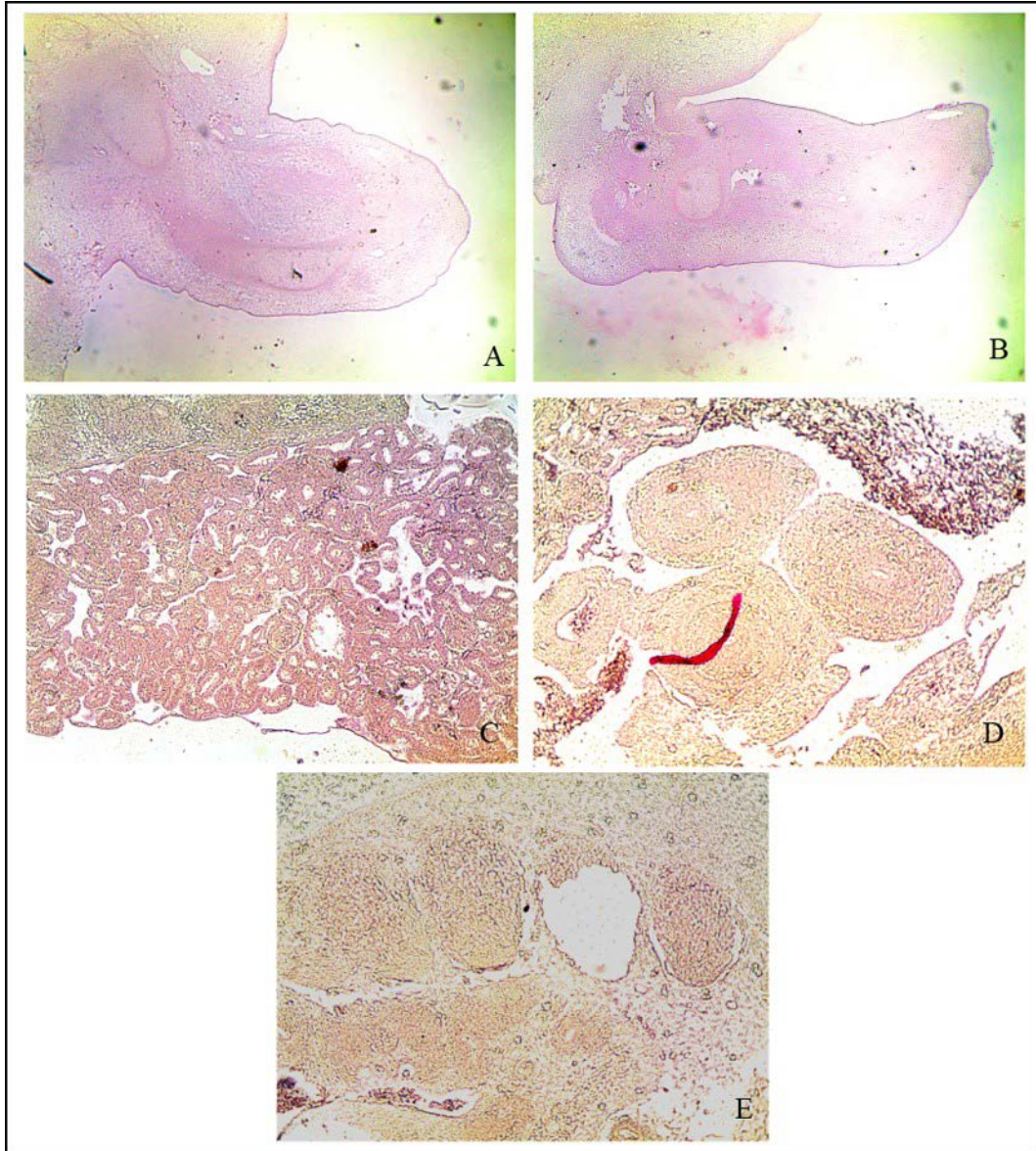


**Figure 22:** Antibody control group of immunostaining of COX-2 confirming the absence of non-specific staining. A: forelimb of day-5 embryo. B: hindlimb of day-5 embryo. C: kidney of day-6 embryo. D: testis of day-7 embryo. E: somites of day-9.

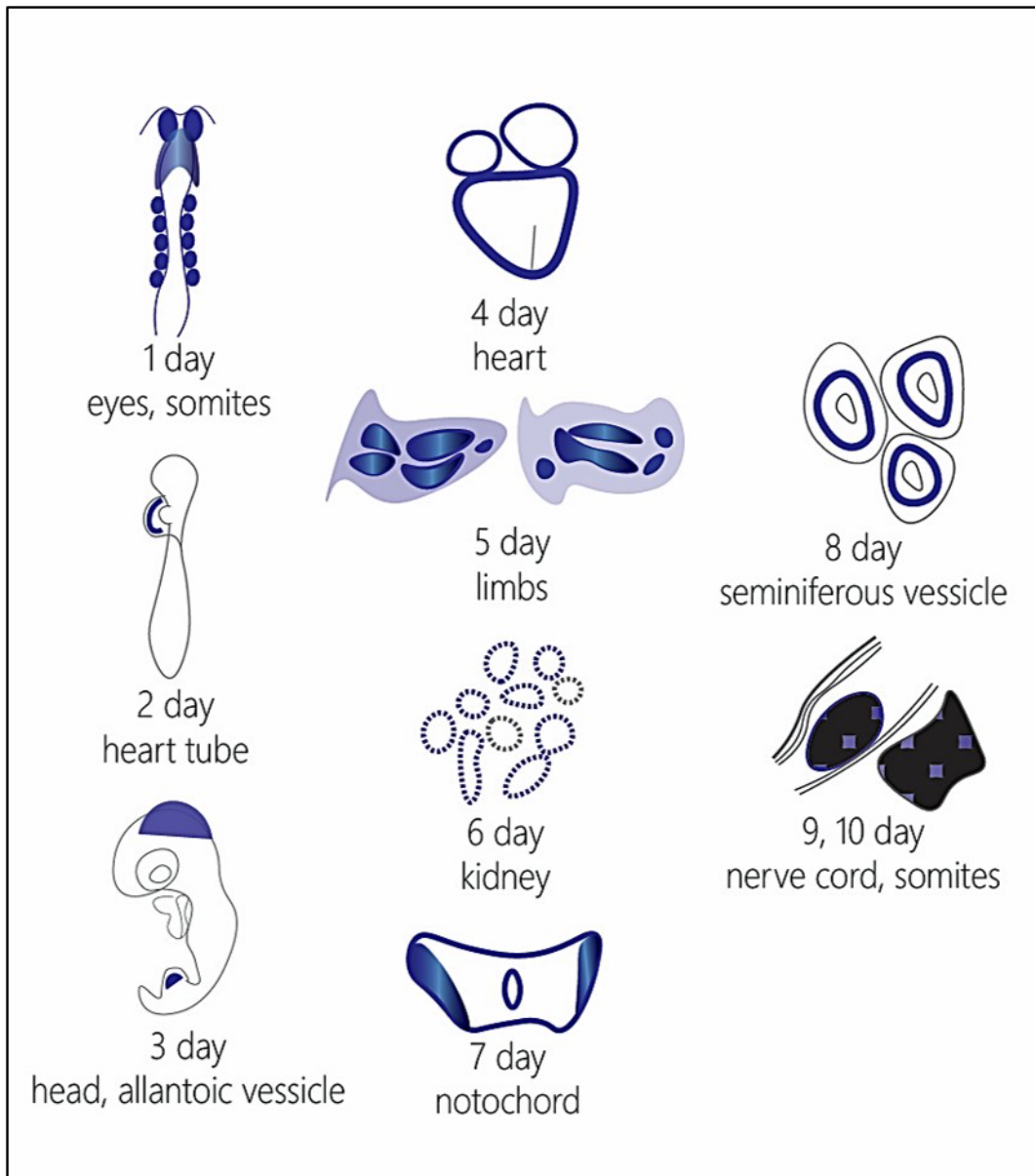


**Figure 23:** Graphical summary of COX-2 localization areas shown with the help of blue coloration in various tissues of chick embryos.